Design and synthesis of 2-Substituted-4-benzyl-5-methylimidazoles as new potential Anti-breast cancer agents to inhibit oncogenic STAT3 functions

Botros Y. Beshay [a,1], Amira A. Abdellatef [b,1], Yasser M. Loksha [c], Salwa M. Fahmy [d], Nargues S. Habib [d], Alaa El-Din A. Bekhit [e], Paris E. Georghiou [f], Yoshihiro Hayakawa [b,*], Adnan A. Bekhit [d,g,h,*]

[a] Department of Pharmaceutical Chemistry, College of Pharmacy, Arab Academy for Science, Technology and Maritime Transport, Alexandria, Egypt
[b] Section of Host Defences, Institute of Natural Medicine, University of Toyama, Toyama, Japan
[c] Department of Pharmaceutical Chemistry, Faculty of Pharmacy, Sinai University, Al-Arish, North Sinai, Egypt
[d] Department of Pharmaceutical Chemistry, Faculty of Pharmacy, Alexandria University, 2152 Alexandria, Egypt
[e] Department of Food Science, University of Otago, Dunedin, New Zealand
[f] Department of Chemistry, Memorial University of Newfoundland, St. John's, NL, Canada
[g] Pharmacy Program, Allied Health Department, College of Health and Sport Sciences, University of Bahrain, Bahrain
[h] Cancer Nanotechnology Research Laboratory (CNRL), Faculty of Pharmacy, Alexandria University, Alexandria 21521, Egypt

ARTICLE INFO

ABSTRACT

STAT3 signaling is known to be associated with tumorigenesis and further cancer cell-intrinsic activation of STAT3 leads to altered regulation of several oncogenic processes. Given the importance of STAT3 in cancer development and progression particularly breast cancer, it is crucial to discover new chemical entities of STAT3 inhibitor to develop anti-breast cancer drug candidates. Herein, 4-benzyl-2-benzylthio-5-methyl-1*H*-imidazole (**2a**) and 4-benzyl-5-methyl-2-[(2,6-difluorobenzyl)thio]-1*H*-imidazole (**2d**) from a group of thirty imidazole-bearing compounds showed greater STAT3 inhibition than their lead compounds VS1 and the oxadiazole derivative MD77. Within all tested compounds, ten derivatives effectively inhibited the growth of the two tested breast cancer cells with IC_{50} values ranging from 6.66 to 26.02 μM. In addition, the most potent derivatives **2a** and **2d** inhibited the oncogenic function of STAT3 as seen in the inhibition of colony formation and IL-6 production of breast cancer cell lines. Modeling studies provided evidence for the possible interactions of the synthesized compounds with the key residues of the STAT3-SH2 domain. Collectively, our present study suggests 2-substituted-4-benzyl-5-methylimidazoles are a new class of anti-cancer drug candidates to inhibit oncogenic STAT3 function.

1. Introduction

Signal transducers and activators of transcriptions (STATs) are a group of latent cytoplasmic proteins that play a crucial physiological role to be activated by extracellular ligands such as cytokines, growth factors, and hormones. Several recent reviews on STATs comprehensively highlight their diverse roles [1-5] and the importance of the Janus tyrosine kinases (JAKs) for their activation [6,7]. In general, phosphorylated STATs form homo- or hetero-dimers are translocated to the nucleus where they regulate the target genes expression through their transcriptional activities [5]. To date, seven members of the STAT family have been identified in mammals [6-8]. The activation of STATs in normal cells is tightly regulated in order to maintain homeostatic regulation of their target gene expression, however, the aberrant activation of STATs in cancer cells has been widely known. Among various STAT family members, JAK-STAT3 signaling is known to associate with tumorigenesis [6,7] and further cancer cell-intrinsic activation of STAT3 leads to altered regulation of several oncogenic processes such as proliferation, cell cycle progression, apoptosis, angiogenesis, metastasis, and immune evasion [9-11]. The cell-intrinsic activation of STAT3 has

---

been found in many different types of malignancies, such as head, neck, breast, prostate, skin, and pancreatic cancers [12-16].

Given the importance of STAT3 in cancer, many studies have been conducted to discover new chemical entities of STAT3 inhibitor by understanding of the binding to the active site(s) of STAT3 protein using computational simulations and structural modification [17-20]. While many approaches have considered different protein domains on STAT3 to design high potent and selective inhibitors of STAT3, the majority of STAT3 inhibitors were designed to target the SH2 domain of STAT3 which regulates the phosphorylation-induced protein dimerization step [21-25]. Upon STAT3 dimerization, the molecular interface is formed between the SH2 domains and the two carboxyl transcription activation domains to stabilize the dimer and lead to the phosphorylation of Tyr705 in a specific pocket of the SH2 domain. The conserved arginine residue in all known SH2 domains (Arg609 in STAT3) are located in the interior of the SH2 domain and represents the key element for the p-Tyr705 recognition [20]. Considering this arginine residue stabilizes the p-Tyr705 binding by forming an energetically-favorable electrostatic interaction between the negatively charged phosphate and the positive NH-phosphorylated STAT3, the competitive compounds for the binding of p-Tyr705 to the SH2 domain of STAT3 has been structurally optimized to synthesize potential STAT3 inhibitors [24,26,27].

A systematic STAT3–SH2 binding site analysis was later conducted by Poli and coworkers [28] who developed a structure-based pharmacophore model by considering the protein–protein interactions previously identified in the STAT3 dimer involving the pTyr705 and Leu706 residues of the phosphopeptide of one monomers with the residues of the of the SH2 domain of the other monomer. The resulting pharmacophore model which they constructed included the following four components: (i) an electron-withdrawing region to represent the pTyr705 phosphate group; (ii) an aromatic component representing the pTyr705 aromatic ring; (iii) a hydrogen-bonding component representing the interaction of the amide N—H moiety of Leu706 with Ser636, a second phosphorylation site in the C-terminal domain of the STAT structure; and (iv) a hydrophobic region representing the Leu706 lateral chain. Their study resulted in the finding of a non-peptide thiourea-based STAT3-SH2 inhibitor, VS1 (Fig. 1) [28]. This molecule exhibited good STAT3 inhibitory activity and was compared with the more highly potent STAT3 inhibitor lead compound, MD77 (Fig. 1) [26,27]. Besides, several studies have introduced compounds bearing-imidazole ring as an important scaffold in drug discovery, particularly as anti-cancer agents. Recently, certain number of imidazole-based compounds including dacarbazine, temozolomide, zoledronic acid, and mercaptopurine are being used in clinical trials for cancer patient treatment [29].

The objective of the present work was to optimize the affinity of the structurally different lead compounds VS1 and MD77 with the insertion of imidazole scaffold, through the application and synthesis of different drug design strategies. Ring-closure of the thiourea moiety of VS1 afforded a series of more rigid imidazole derivatives which, together

with the bioisosteric replacement of the 1,2,5-oxadiazole scaffold which is present in MD77, with an imidazole ring, the new target compounds A-F were conceived. Furthermore, the present work also aimed to study the effect of having different spacers between the imidazole scaffold and the hydrophobic moiety at C2. The proposed candidates which were designed and synthesized (Fig. 2) comprised the key four pharmacophore features established by the receptor-based pharmacophore model constructed by Poli et al. [28]. These newly synthesized compounds were screened for their anti-proliferative activity against triple-negative breast cancer cell lines.

2. Results and discussion

2.1. Synthesis of the target compounds

The Dakin-West reaction was used to prepare the imidazole-2-thione **1** (Scheme 1) from *d,l*-phenylalanine [30-32]. This imidazole-2-thione derivative **1** is the key precursor compound for the synthesis of the target imidazole derivatives **2a-e**, **3–5**, **6a-b**, and **7a-h** (Schemes 1-3).

As shown in Scheme 1, the desired 2-arylmethylthio-4-benzyl-5-methyl-1*H*-imidazoles (**2a-e**) were obtained by the potassium carbonate-mediated coupling of 4-benzyl-5-methyl-1,3-dihydro-2*H*-imidazole-2-thione **1** and the respective benzylbromide derivatives in acetone. Previously, Loksha et al. [31] were able to synthesize **2a** in 26% yield by the coupling of **1** with benzyl bromide in the presence of potassium carbonate in *N,N*-dimethylformamide (DMF). In the present investigation, **2a** was easily obtained in a much higher yield (90%) using acetone as the solvent.

It is worth noting that compound **2b** showed a doubling of the signals of both hydrogen and carbon atoms in its ^{1}H NMR and ^{13}C NMR spectra. This can be explained by the imidazole ring tautomerism, (Fig. 3) that has been shown to cause the disappearance of some carbon signals of the imidazole and aliphatic carbons in several other reported compounds [31].

The coupling reactions of thiols with aryl halides generally require harsh reaction conditions using solvents such as ethanol heated under reflux, or DMSO at 90 °C [33,34]. Rout et al. [35] reported that CuI could efficiently catalyze the C—S cross-coupling of thiols with aryl halides in the presence of tetra-*n*-butylammonium bromide (TBAB) in water. In the current work, the high reactivity of the nitroaryl halide derivatives facilitated the C—S cross-coupling reaction due to the strong electron-withdrawing nitro group substituent(s) in the *ortho* and/or *para* position(s). Thus, the coupling reaction of 4-benzyl-5-methylimidazole-2-thione **1** (Scheme 2) with 1-chloro-2,4-dinitrobenzene was achieved using potassium hydroxide in methanol at rt. However, the synthesis of 4-benzyl-5-methyl-2-((2-nitrophenyl)thio)-1*H*-imidazole **4** required the use of a strong base, sodium hydride, in DMF.

Direct coupling of **1** with phenacyl bromide derivatives in ethanol using the reported procedure [36] did not afford the desired 2-aroyl-methythio-4-benzyl-5-methyl-1*H*-imidazoles **6a, b** in good yields, even
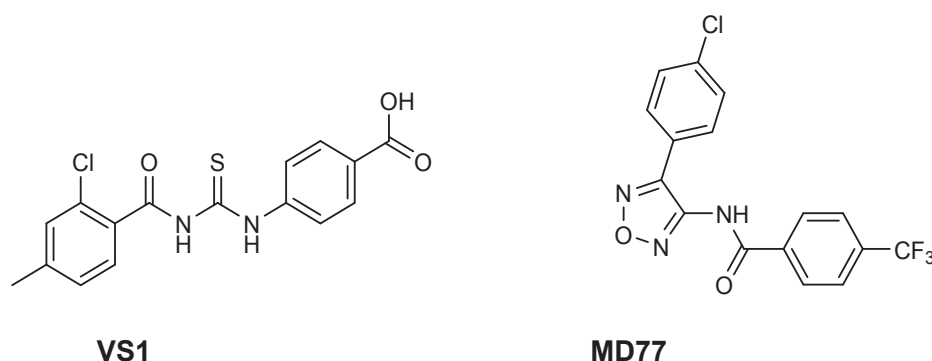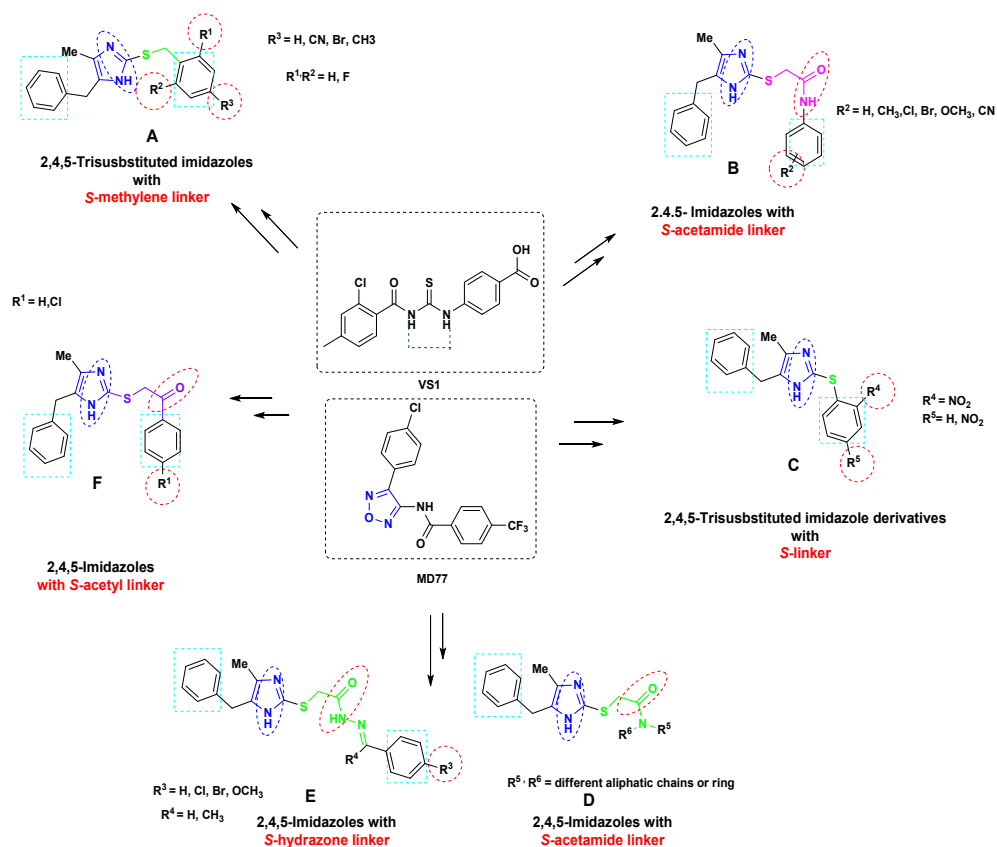
Fig. 1. Chemical structures of lead compounds VS1 and MD77.

Fig. 2. Design of 2,4,5-trisusbstituted imidazole derivatives A-F connected to aryl moieties with different small electron-withdrawing groups *via* *S*-methylene, sulfur, *S*-hydrazone or *S*-acetyl linkers. The red circles or ovals refer to electron withdrawing features. The blue ovals refer to H-bond donor features and the cyan squares refer to the aromatic and hydrophobic features. Different spacers are highlighted by different colors. (For interpretation of the references to colour in this figure legend, the reader is referred to the web version of this article.)

2	R^1	R^2	R^3
a	H	H	H
b	H	H	Br
c	H	H	CN
d	F	F	H
e	H	H	CH$_3$
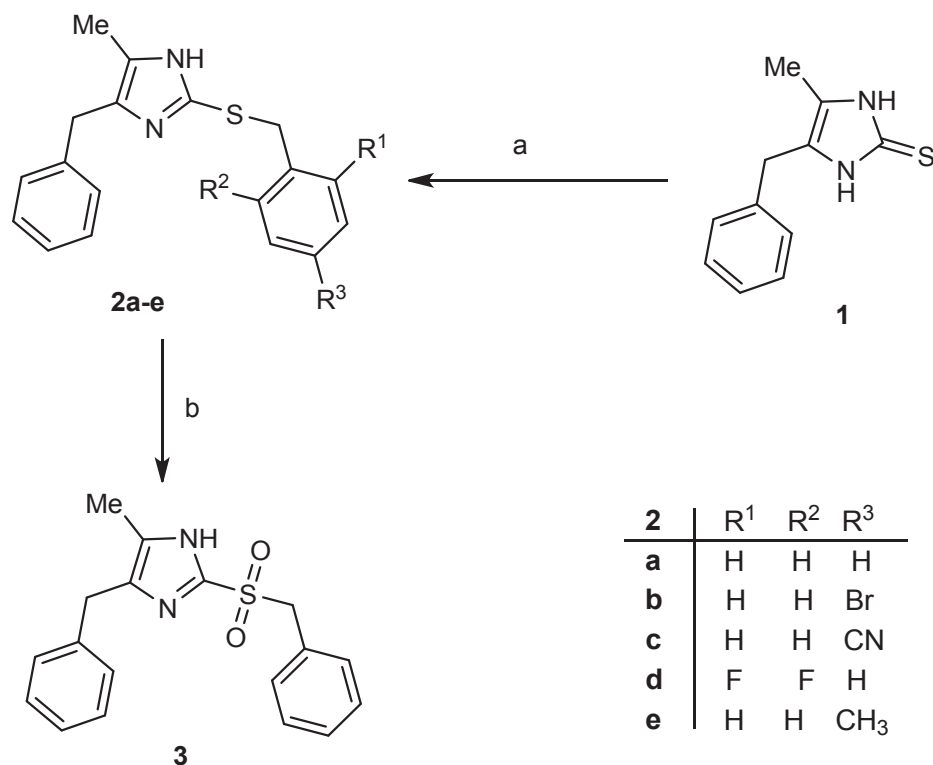
Scheme 1. Reagents and conditions: (a) ArCH$_2$Br, K$_2$CO$_3$, acetone, rt, 8 h (b) **2a**, H$_2$O$_2$, EtOH, 60 °C, 24 h.
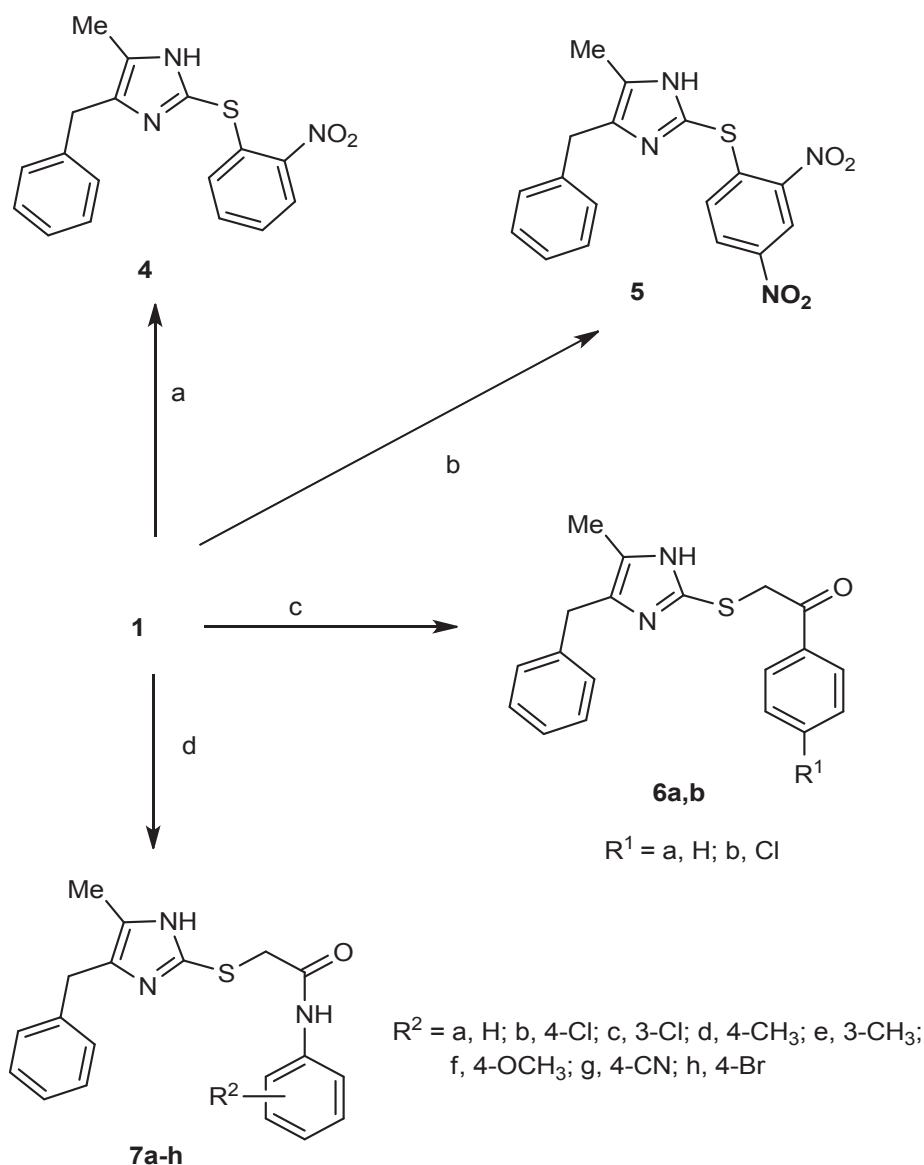
Scheme 2. Reagents and conditions: (a) 2-nitrofluorobenzene, NaH, DMF, rt, 12 h (b) 2,4-dinitrochlorobenzene, MeOH, KOH, rt, 6 h (c) ArCOCH$_2$Cl, NaH, DMF, rt, 3 h (d) ArNHCOCH$_2$Cl, NaH, DMF, rt, 3 h.

using different conditions including the use of potassium carbonate in DMF; potassium carbonate in acetone, triethylamine in DMF, or sodium hydride in DMF. The most convenient method that also gave the highest yields of **6a** (92%) and **6b** (89%) within a short time (2 h) was the use of sodium hydride in DMF under anhydrous conditions, at rt.

The substituted chloroacetanilide derivatives, which were required for the preparation of compounds **7a-h**, were prepared from the corresponding aniline derivatives and chloroacetyl chloride [37] at rt under basic anhydrous DMF conditions with trimethylamine. *S*-alkylation of these chloroacetanilide derivatives with **1** to form the corresponding products **7a-h** was achieved in excellent and reproducible yields (85–94%) using sodium hydride in DMF at rt for short reaction times (2 h). Other researchers [38] described *S*-alkylation reactions of thiols with chloroacetanilide derivatives in 70% yields using DMF containing tri-methylamine under reflux conditions, but here we found the use of sodium hydride was optimal.

The synthesis of ethyl 2-[(4-benzyl-5-methyl-1*H*-imidazol-2-yl) thio] acetate **8** (Scheme 3) was accomplished in a pure and crystalline state by the *S*-alkylation reaction of **1** with ethyl chloroacetate in anhydrous acetone and potassium carbonate. With compound **8** in hand, the

corresponding *N,N*-dimethylamide **9**, cyclohexylamide **10a**, and 2-*N,N*-dimethyl)-*N*-ethylamide **10b** were synthesized cleanly from the corresponding primary and secondary aliphatic amines using a modification of a reported procedure [38]. A higher boiling point solvent such as dioxane, and varying reaction times from 24 to 48 h, according to the reactivity of the amines was required for these amides.

The corresponding acid hydrazide **11** was obtained by heating ester **8** with an excess amount of hydrazine in ethanol under reflux using the procedure described by Salman et al. [38]. Despite, the target hydrazone derivatives **12a-g** were prepared from the acid hydrazide by a condensation reaction of the appropriate aldehydes and ketones in ethanol in the presence of a few drops of glacial acetic acid [39]. All desired hydrazones precipitated out from the reaction mixture after few hours, while compound **12e** precipitated out only after pouring the reaction mixture onto ice-cold water.
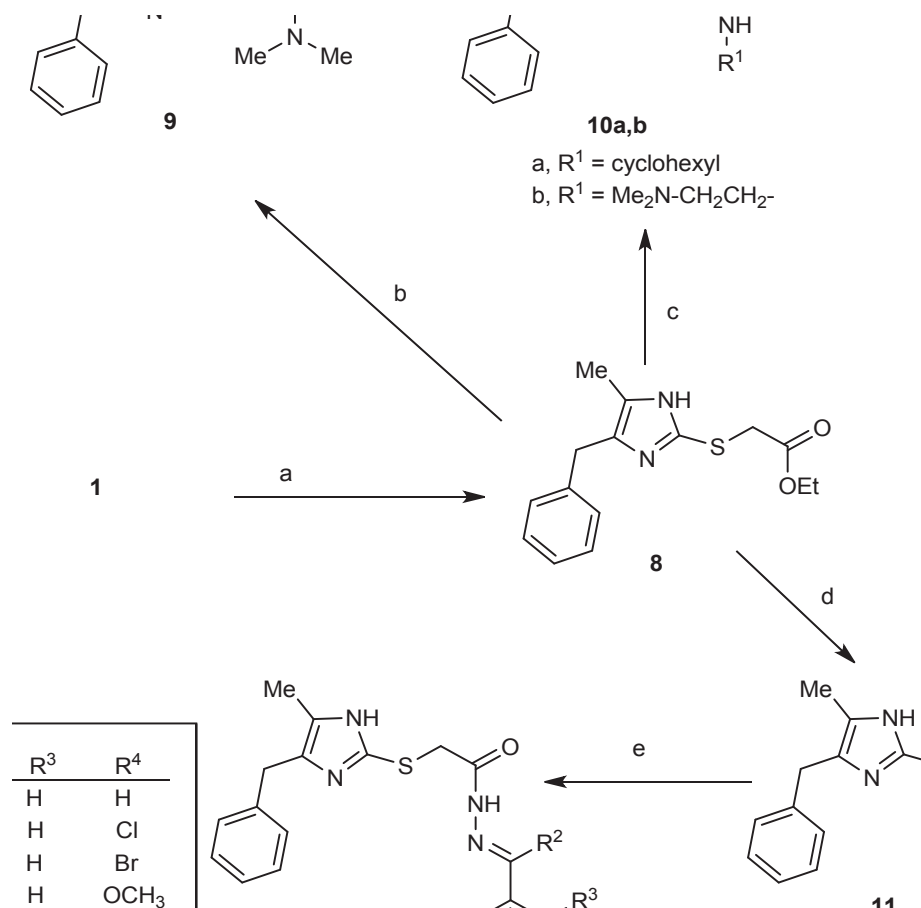
Scheme 3. Reagents and conditions: (a) Cl-CH$_2$COOEt, K$_2$CO$_3$, acetone, rt, 6 h (b) Me$_2$NH, 1,4-dioxane, reflux, 36 h (c) R-NH$_2$, 1,4-dioxane, reflux, 24–48 h (d) N$_2$H$_4$·H$_2$O, ethanol, 60 °C, 6 h (e) aromatic aldehydes or ketones, acetic acid, ethanol, rt, 6–24 h.
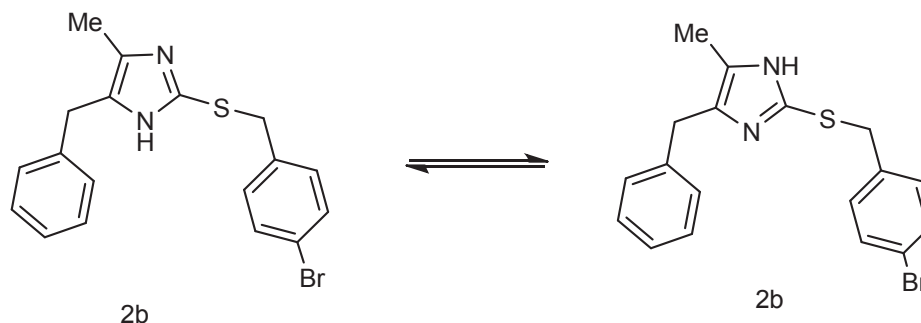
Fig. 3. The imidazole ring tautomers of 2b.

2.2. Biological screening

2.2.1. Anti-tumor activities of synthesized imidazole derivatives against breast cancer cells.

MD77 and VS1 are previously reported as STAT3 inhibitors directly targeting its SH2 domain [26-28], however, their potency needs to be improved. Therefore, we conducted the screening of the newly synthesized imidazole derivatives for their anti-tumor effect on breast cancer cell lines, 4 T1, and MDA-MB-231 in which STAT3 is over activated. The summary of IC$_{50}$ values is shown in Table1. Among thirty tested imidazole derivatives, a group of ten compounds showed varying degrees of anti-cancer activities. While there are compounds with low (**2e**, **7e**) or moderate (**4, 5, 7a, 7c, 12a, 12e**) activity, the two compounds (**2a, 2d**) with the *S*-methylene linkers of unsubstituted phenyl ring (**2a**), and 2,6-

Table 1

In vitro anti-tumor activity of tested imidazole derivatives on breast cancer cell lines.

Compound ID	IC$_{50}$ values (μM)	
	4 T1-Luc2	MDA-MB-231
2a	8.03	8.26
2d	6.66	9.50
2e	17.98	10.83
4	8.73	13.88
5	7.04	7.70
7a	10.44	13.47
7c	15.99	8.11
7e	26.02	10.43
12a	10.42	14.38
12e	10.86	10.54
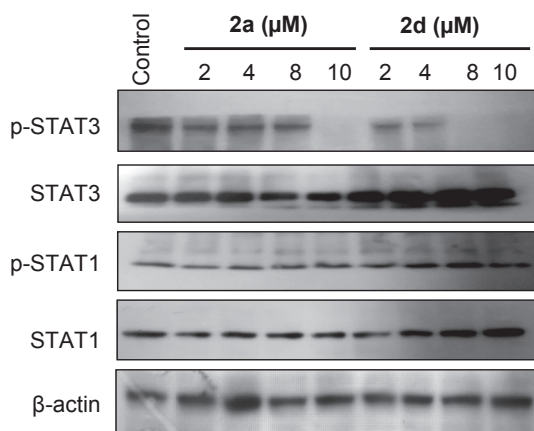
Fig. 4. Inhibition of phosphorylated-STAT3 and STAT1 by the target compounds 2a and 2d. 4 T1 cells (1x10^6 cells/well) were pre-treated with **2a** or **2d** (DMSO vehicle, 2, 4, 8, 10 μM) for 6 h. Whole-cell lysates were immuno-blotted with anti-STAT3, p-STAT3 (Tyr705), STAT1, p-STAT1 (Tyr701) antibodies. β-actin was used as the loading control.

difluorophenyl ring (**2d**) showed the potent anti-tumor effect on the tested cell lines.

2.2.2. Imidazole derivatives 2a and 2d suppressed STAT3 phosphorylation and its oncogenic functions.

To examine whether **2a** and **2d** inhibit STAT3 activity, the effects of **2a** and **2d** on the phosphorylation of STAT3 in 4 T1 cells were evaluated. As shown in Fig. 4, both **2a** and **2d** treatment inhibited the expression of phosphorylated STAT3 at Tyr705 in a dose-dependent manner without affecting the total expression of STAT3. Considering the expressions of both STAT1 and phosphorylated STAT1 were not affected by **2a** or **2d** treatment, the primary target of **2a** and **2d** should be specific to STAT3. Such specificity of **2a** or **2d** to STAT3 inhibition is contrary to MD77, which is known to inhibit both STAT3 and STAT1 with IC$_{50}$ 17.7 and 7.2 μM, respectively [28]. Furthermore, in *silico* docking studies revealed that a number of compounds with STAT3 inhibitory activity often show STAT1 inhibition [40,41]; therefore, the selectivity of **2a** and **2d** on STAT3 might be an advantage to the other known compounds.

To further determine the significance of **2a** and **2d** on their inhibition on the oncogenic STAT3 function, we tested **2a** and **2d** on the *in vitro* colony formation of 4 T1 and MDA-MB-231 breast cancer cell lines. As shown in Fig. 5, both **2a** or **2d** pre-treatment reduced the colony formation of 4 T1 and MDA-MB-231 cells. Furthermore, **2a** and **2d** also inhibited the production of IL-6 from 4 T1 cells, which is known to be a pro-tumorigenic cytokine to activate STAT3. Collectively, these data strongly suggest those **2a** and **2d** as 2-substituted-4-benzyl-5-methylimi-dazoles are novel class of synthetic anti-breast cancer compounds by inhibiting oncogenic STAT3 activity (see Fig. 6).

2.2.3. Structure-activity relationship of synthesized compounds.

The obtained results indicated that an imidazole scaffold with different spacer groups resulted in diverse effects on the *in vitro* anti-tumor activity. The results can be summarized as follows: (i) The imidazole derivatives **2a** and **2d** with *S*-methylene linkers showed the strongest activities. (ii) The presence of the small electron-donating methyl group on the *para*-position of the benzyl moiety in **2e** appeared to slightly decrease the anti-tumor activity. It was evident also that the presence of the large electron-withdrawing groups (bromo or cyano groups) on the benzyl moiety abolished the activity of compounds **2b** and **2c**. The presence of a sulphonyl-methylene linker in **3** formed by the oxidation reaction of **2a** (Scheme 1) led to the loss of the inhibitory activity against the tested cell lines. (iii) The imidazole candidates having only a sulfur atom linker showed good inhibitory activity on the tested cell lines, with the dinitro-substituted derivative **5** exhibiting

greater activity than the mono-substituted derivative **4**. Based on these results, a clear structure and activity relation could be concluded wherein the insertion of small linkers such as a sulfur atom or a *S*-methylene group, directly attached to an aromatic ring with small-sized electronegative substituents in the target compounds **2a** and **2d** seem to be necessary for the potent activity.

Replacing the *S*-methylene linker with the longer *S*-acetamide spacer decreased the inhibitory activity (8.11–26.02 μM). Among the *S*-acet-amide linker-diaryl-substituted imidazole derivatives, **7c** showed high anti-tumor activity on MDA-MB-231 cells, with IC$_{50}$ = 8.11 μM. The substitution of the phenyl ring, which is attached to the *S*-acetamide linker, with small electron-donating or withdrawing groups at the *meta*-positions slightly decreased the activity as shown in compound **7c**. However, the substitution of the phenyl ring at the *para*-positions abolished the activity of the other compounds (**7b, 7d, 7f-h**) in this series. It is clear that the presence of nitro or fluoro substituents plays a pivotal role in enhancing the potent activity of the tested cells. The introduction of *S*-hydrazone spacers led to a remarkable decline in the anti-tumor activity of imidazole derivatives **12a-g**, except for candidates **12a** and **12e** which maintained their anti-tumor activity. While **12a** exhibited preferential cytotoxic activity on 4 T1 cells with IC$_{50}$ = 10.42 μM, **12e** showed the highest potency on MDA-MB-231 cells with IC$_{50}$ = 10.54 μM.

It is also clear that the replacement of the arylhydrazone moiety with different open-chain and cyclic aliphatic fragments markedly abolished the anticancer potency of imidazole derivatives **8, 9, 10a-b,** and **11**. These results highlight the importance of the aromatic ring, which is attached to *C*2 of the imidazole ring, for maintaining the inhibitory activity against breast cancer cells.

2.3. Molecular Modeling

A docking study was performed into the binding site of STAT3-SH2 (PDB ID: 1BG1), to compare the mechanism of action of their inhibitory activities and their binding affinities to the protein active site relative to the lead compounds VS1 and MD77 [42]. The docking study was performed using Discovery Studio (DS) 5.0 client (Accelrys) [43]. The selection of the docking poses generated with CDOCKER, which is a grid-based docking program within the DS software, was based upon the conformation with the highest score and the best binding interactions. In addition, binding energy scores (CDOCKER energy), and the formation of hydrogen bonds with the conserved amino acid residues were the factors determining the binding affinities to the binding pockets of the selected proteins.

The most active compounds (**2a** and **2d**) were examined for their top-scored binding with the best binding affinities and they were found to bind at the active site with better scoring than lead compound VS1 and were comparable to MD77, with hydrophilic and hydrophobic types of interactions comparable to those shown with the lead compounds (Table 2) [26-28].

Examination of the best-docked poses of imidazole derivative **2a** (Fig. 7) revealed that it was perfectly positioned in the active site of STAT3-SH2 with a scoring energy of −20.12 kcal/mol. The nitrogen atom of the imidazole fragment of compound **2a** displayed the corner-stone hydrogen bonds with the amine functionalities of Arg609. This amino acid contributed markedly to STAT3 and SH2 peptide binding, as the mutation of Arg609 has been shown to abolish the peptide-binding ability of this domain [44,45]. Furthermore, the hydrogen bonds with Ser613 (two hydrogen bonds), Glu612, and other electrostatic forces with Lys591 (δ-cation), Pro639 (δ-alkyl) also enhanced the blocking of the STAT3-SH2 binding site.

Additionally, the sulfur atom of the *S*-methylene linker forms two hydrogen bonds with the NH back-bone of Glu612 and Ser611. The imidazole scaffold NH forms a strong hydrogen bond with Ser613. Additionally, strong electrostatic interactions of the δ-cation type are formed between the δ-cloud of the imidazole ring and the NH$_3^+$ group of

Concentration 10 μM

MDA-MB-231

4T1-Luc2

Control

2a

2d
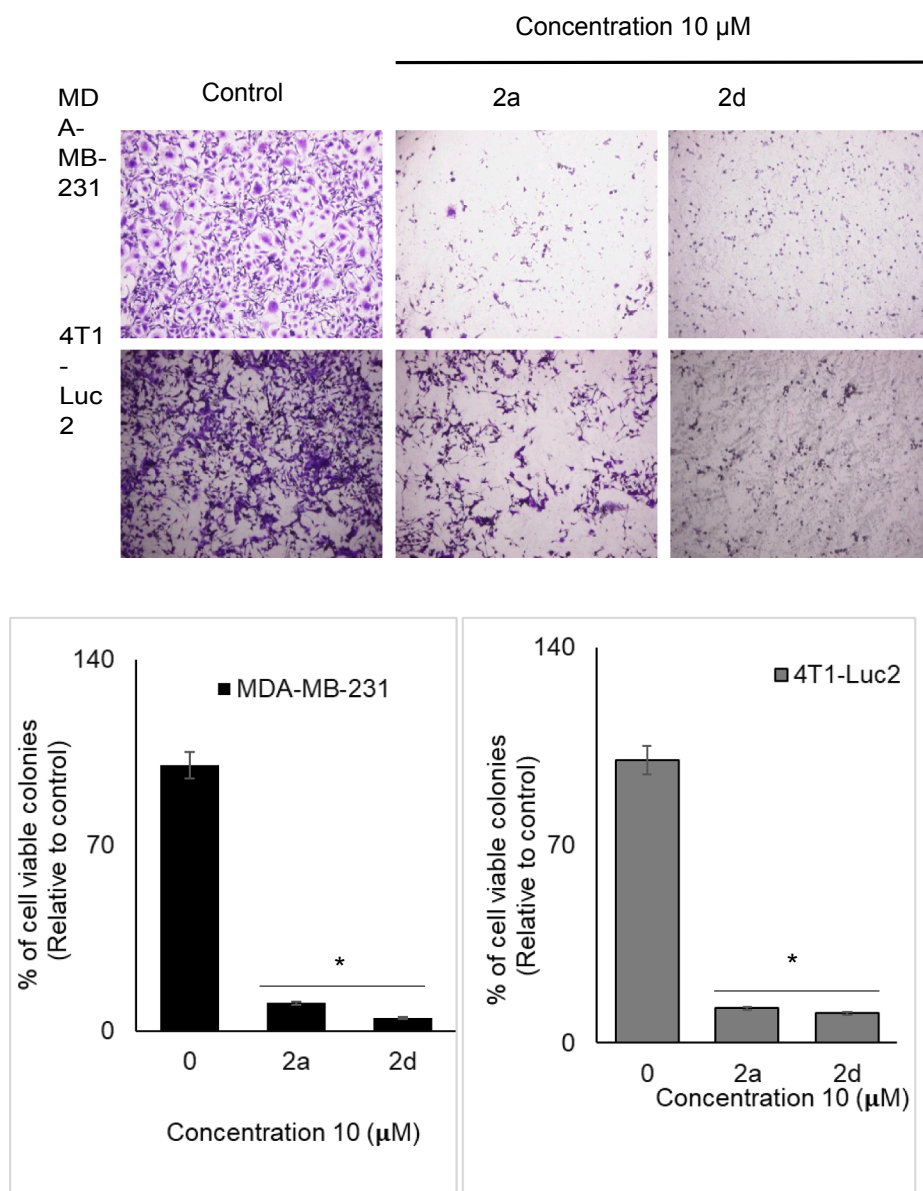
Fig. 5. Inhibition of the colony formation by the target compounds 2a and 2d. 4 T1 and MDA-MB-231 cells were treated with **2a** or **2d** (10 μM) or with the vehicle for 24 h, then the number of formed cell colonies was counted 10 days after seeding. Data are expressed as colony-forming efficiency calculated as a percentage with respect to control cells. The representative images of colonies formed (upper panel) and the summaries of number of formed cell colonies (lower panel) are presented. The data are presented as the mean ± SD.

Lys591. The binding mode of **2a** is comparable to p-Tyr705 because it involves the same pocket into which p-Tyr705 is inserted when the two STAT3 subunits are assembled in the dimer. This pocket is placed on the protein surface and is surrounded by hydrophilic and polar amino acids to better interact with the negatively-charged side-chain of the phosphorylated tyrosine, which is mimicked by the benzylthiomethylimidazole moiety.

The docking results obtained for **2d** revealed a good binding pattern in the active site of STAT3-SH2 with a binding energy score of −17.22 kcal/mol. The binding mode of **2d** showed that the two nitrogen atoms of the imidazole conserved the crucial hydrogen bonds with Arg609 and Ser613. Additionally, one of the fluorine atoms at an *ortho* position of the 2,6-diflurobenzyl fragment forms an intramolecular hydrogen bond with the NH of the imidazole scaffold, which also forms a strong hydrogen bond with Ser613. We can presume that these bridged hydrogen bonds are also crucial for maintaining the STAT3 inhibitory activity of **2d**. Additionally, the decreased STAT3 inhibitory activity of **2d** in comparison with **2a** could be explained by the loss of the additional hydrogen bonds formed with Ser613, Glu612, and the electrostatic interactions with Pro639 (Fig. 8).

2.4. Optimization measures

2.4.1. Ligand Efficiency (LE) and (Ligand Lipophilic Efficiency) LLE

As shown in Table 3, the most active compounds fall within the acceptable Ligand Efficiency (LE) and (Ligand Lipophilic Efficiency) LLE ranges [46-48]. Compounds **2a**, **2d**, and **5** showed LE values ranged between 0.74 and 0.95. In terms of lipophilicity, compounds **2a** and **2d** exhibited LLE values of 9.82 and 7.47, respectively. Amongst all tested compounds, **2a** and **2d** presented the optimum values (LE > 0.3, LLE > 5), which possessed the best drug-like criteria along with significant potency as promising anti-cancer agents.

3. Conclusions

Our approach in designing imidazole derivatives as potential new anti-cancer agents was successfully accomplished and the results can be summarized as follows: All newly synthesized compounds revealed moderate-to-potent anti-tumor activity against breast cancer cells. Imidazole derivatives with *S*-methylene linker **2a** and **2d** exhibited the most potent anti-tumor activity. Specifically, compound **2d** had IC$_{50}$ values of 6.66 and 9.50 μM against 4 T1 and MDA-MB-231 cells,
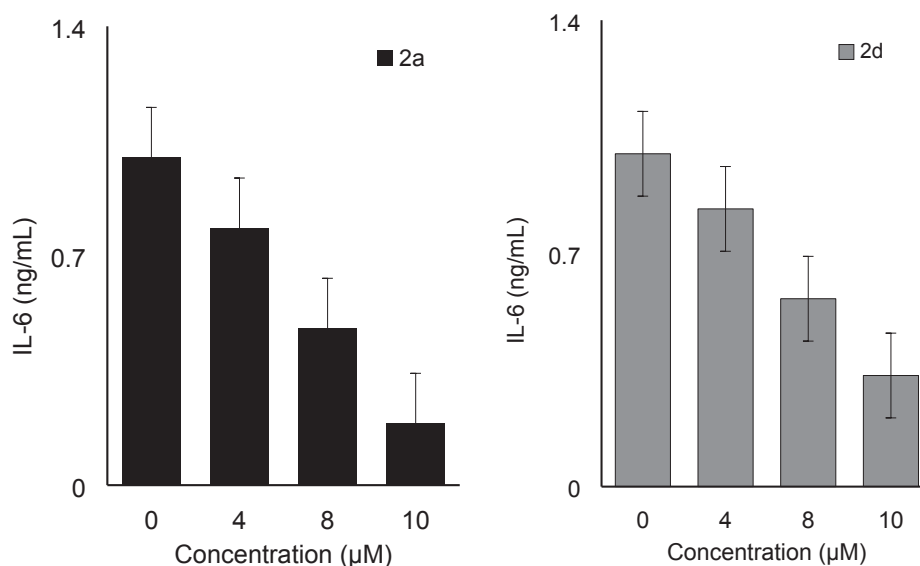
Fig. 6. Suppression of the pro-inflammatory cytokine IL-6 by the target compounds 2a and 2d. 4 T1-Luc2 cells ($2x10^5$ cells/well) were incubated with **2a** or **2d** (DMSO vehicle, 4, 8, 10 μM) for 24 h at 37 °C, and the level of IL-6 were then determined in the cell-free culture supernatants by ELISA. The data are presented as the mean ± SD.

Table 2

Binding score and the detailed interactions of the target compounds 2a and 2d in the active site of STAT3-SH2.

Comp. No.	Binding score (kcal/mol)	H-bonding Interactions	Electrostatic Interactions	Hydrophobic Interaction
VS1	−12.3	Ser611, Ser612, Ser613, Ser636		Thr620, Trp623, Gln635, Glu638, Pro639, Val637, Tyr657, Thr714, Phe716
MD77	−18.56	Arg595, Lys591, Arg609, Gln635		Arg595, Gln635
2a	−20.12	Arg609, Ser613, Glu612	Lys591, Pro639	Lys557, Lys591, Ser611, Ser636, Val637, Glu638,
2d	−17.22	Arg609, Ser613	Lys591	Lys557, Lys591, Glu594, Ser611, Glu612, Ser613, Thr620, Ser636, Val637, Glu638

respectively, and compound **2a** showed IC_{50} values of 8.03 and 8.26 μM against the same cell lines. Compounds **2a** and **2d** displayed excellent p-STAT3 inhibitory activity compared to the lead compounds VS1 and MD77. The most potent compounds were further examined *in vitro* for suppressing the oncogenic functions of STAT3 which were recognized by inhibiting the pro-inflammatory cytokine IL-6 and suppressing the colony formation of breast cancer cells.

The docked models obtained for these active molecules revealed excellent binding profiles in the active site of STAT3-SH2 (PDB: 1BG1). Good scoring values in addition to the similarities shown with the lead compounds VS1 and MD77 in the types of interactions have been observed. In addition, the optimization measurement tools as LE and LLE revealed that the imidazole derivatives **2a** and **2d** had optimum results (LE > 0.3, LLE > 5) as promising anti-cancer agents. It is worthmentioning, structures of these two compounds suggest that their diarylsubstituted imidazole structure has a small *S*-methylene group linker and which have strong electron-withdrawing groups i.e. fluorine or nitro on the *S*-methylene-linked aromatic ring are essential for maintaining

the remarkable anticancer activity against breast tumors.

4. Experimental details

4.1. Chemistry

4.1.1. Materials and methods

Starting materials, reagents and solvents were purchased from Sigma-Aldrich, Merck, Acros, Alfa Aeser, and Gomhoria Co. Melting points were determined in open-glass capillaries using a Graffin melting point apparatus and are all uncorrected. The synthetic reactions were monitored by Merck silica gel thin-layer chromatography (TLC) sheets and the spots were visualized with a UV lamp at ë 254 nm. Infrared spectra (IR) were recorded, using KBr discs, υ (cm^{-1}), on a Perkin-Elmer 1430 infrared spectrophotometer, Central Laboratory, Faculty of Pharmacy, Alexandria University. ^{1}H NMR (300 MHz) and ^{13}C NMR (75 MHz) spectra were performed in CDCl$_3$ or DMSO-d_6, on a Bruker AVANCE III instrument at the Department of Chemistry, Memorial University of Newfoundland, St. John's, Newfoundland and Labrador, Canada, as were the HRMS-ESI which were run on an Agilent 1260 Infinity LC-6230 TOF LC/MS spectrometer (LCMS). Microanalyses were performed on Perkin-Elmer 2400 elemental analyzer, and the values found were within ± 0.3% of the theoretical values. Compounds **1** and imidazole derivative **2a** were prepared according to the procedures described by Dakin & West [30] and Loksha et al. [31,32].

4.1.2. 4-Benzyl-5-methyl-1H-imidazole-2(3H)-thione (1).

A mixture of **3** (6.50 g, 32.5 mmol) and potassium thiocyanate (3.10 g, 32.5 mmol) in water (100 mL) was heated under reflux for 3 h. The reaction mixture was cooled and the solid product was isolated by filtration and recrystallized from ethanol/water to give 4.64 g of **1** as pale-yellow crystals; yield 70%; mp 275–279 °C (lit. [31,32] 270–273 °C. ^{1}H NMR (DMSO-d_6) ä [ppm]: 1.98 (s, 3H, CH$_3$), 3.66 (s, 2H, CH$_2$-C4), 7.19–7.31 (m, 5H, H$_{arom.}$), 11.65, 11.69 (s, 2H, 2NH). ^{13}C NMR (DMSO-d_6) [ä ppm]: 9.03 (CH$_3$), 29.48 (CH$_2$-C4), 120.63, 123.35, 126.72, 128.65, 128.88, 139.56, 159.32 (C$_{arom}$, C5, C4 and C2). HRMS-ESI: m/z = 205.0793 (C$_{11}$H$_{13}$N$_2$S, [M + H$^+$]); requires 205.0799.

4.1.3. 2-(Arylmethylthio)-4-benzyl-5-methyl-1H-imidazoles (2a-e).

To a suspension of **1** (0.41 g, 2.0 mmol) in acetone (25 mL), appropriate benzyl bromide derivatives (2.0 mmol) and potassium carbonate
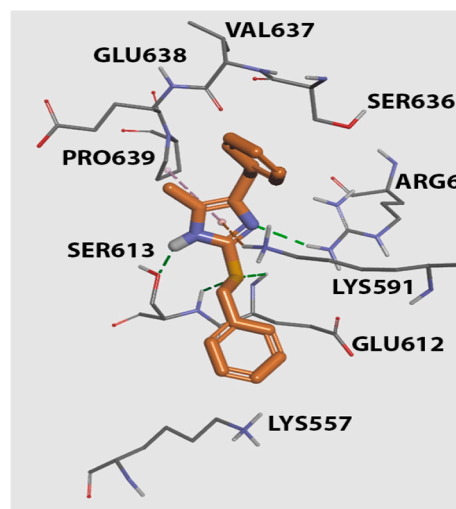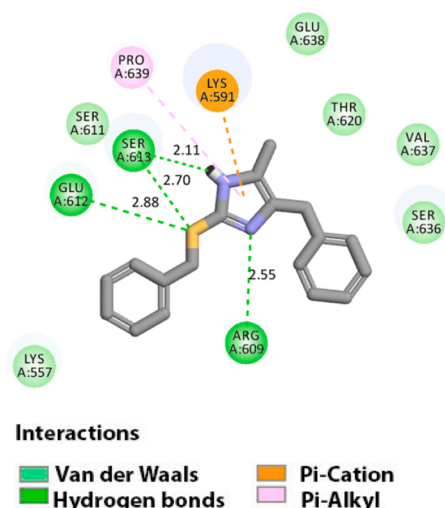
Fig. 7. Docking and binding pattern of compound 2a into the active site of STAT3-SH2. Left and right panels represent the 2D and 3D plots of PDB:1BG1, respectively. Hydrogen bonds are shown with green dotted lines. (For interpretation of the references to colour in this figure legend, the reader is referred to the web version of this article.)
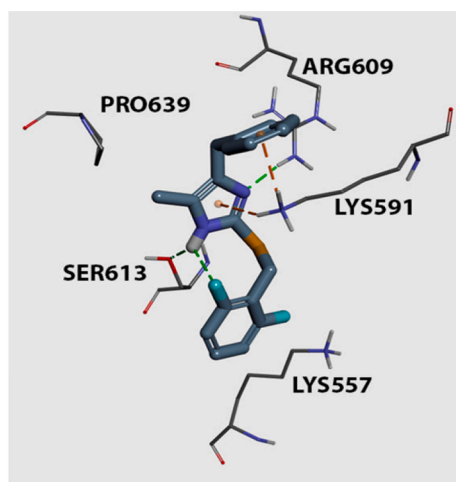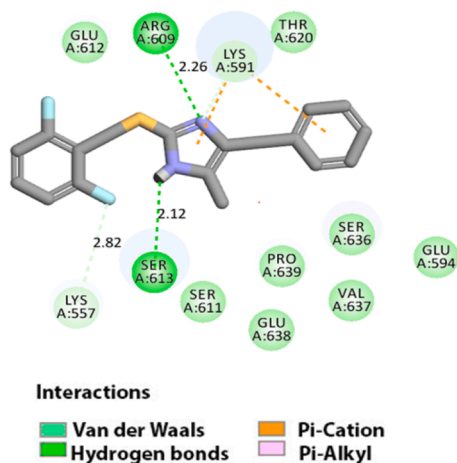
Fig. 8. Docking and binding pattern of compound 2d into the active site of STAT3-SH2. Left and right panels represent the 2D and 3D plots of PDB:1BG1, respectively. Hydrogen bonds are shown with green dotted lines. (For interpretation of the references to colour in this figure legend, the reader is referred to the web version of this article.)

Table 3
LE and LLE values for the active compounds.

Comp. No.	NHA	Log P	Ä G	LE	LLE
2a	21	4.86	20.12	**0.95**	**9.82**
2d	23	5.09	'17.22	**0.74**	**7.47**
5	26	4.64	9.78	**0.76**	2.50

*Bold numbers represent the top LE and LEE values of the tested compounds.

(0.28 g, 2 mmol) were added. The reaction mixture was stirred for 8 h at rt, and then the solvent was removed under reduced pressure. Ice-cold water was added to the residue and the solid thus obtained was filtered, washed with water and crystallized from acetone.

4.1.3.1. 4-Benzyl-2-benzylthio-5-methyl-1H-imidazole (2a).. Colorless crystals; yield 0.53 g (90%); mp 103–105 °C (lit. [31] 105–107 °C). ^{1}H NMR (CDCl$_3$) ä [ppm]: 2.15 (s, 3H, CH$_3$), 3.85 (s, 2H, CH$_2$-C4), 4.08 (s, 2H, S-CH$_2$), 7.12–7.33 (m, 10*H*, H$_{arom.}$). ^{13}C NMR (CDCl$_3$ [ä ppm]: 11.18 (CH$_3$), 31.79 (CH$_2$-C4), 40.28 (S-CH$_2$), 126.31, 127.27, 128.38,

128.51, 128.55, 128.83, 131.05, 134.48, 135.85, 138.09, 141.34 ($_{Carom}$ C5, C4 and *C*2). HRMS-ESI: m/z = 295.1248 (C$_{18}$H$_{19}$N$_2$S, [M + H$^+$]); requires 295.1269.

4.1.3.2. 4-Benzyl-2-[(4-bromobenzyl)thio]-5-methyl-1H-imidazole (2b).. Colorless crystals; yield 0.65 g (88%); mp 160–163 °C. ^{1}H NMR (DMSO-d_6) ä [ppm]: 2.05, 2.08 (2 s, 3H, CH$_3$, tautomeric), 3.72, 3.79 (2 s, 2H, CH$_2$-C4, tautomeric), 4.12 (s, 2H, S-CH$_2$), 7.11–7.22 (m, 3H, H$_{arom}$ at C4), 7.15 (d, J = 8.3 Hz, 2H, H$_{arom}$ at *C*2), 7.27 (t, J = 7.70 Hz, 2H, H3'' & H5'', H$_{arom}$ at C4), 7.41 (d, J = 8.3 Hz, 2H, H3' & H5', H$_{arom}$ at *C*2), 11.84, 11.88 (2 s, 1H, NH, tautomeric). ^{13}C NMR (DMSO-d_6) [ä ppm]: 9.69, 12.88 (CH$_3$, tautomeric), 30.17, 33.03 (CH$_2$-C4, tautomeric), 37.52, 37.67 (S-CH$_2$, tautomeric), 120.53, 126.02, 126.51, 128.50, 128.55, 128.81, 128.86, 131.32, 131.41, 131.55, 131.65, 138.39 (C$_{arom}$). HRMS-ESI: m/z = 373.0380 and 375.0380 (C$_{18}$H$_{18}^{79}$BrN$_2$S, C$_{18}$H$_{18}^{81}$BrN$_2$S [M + H$^+$]); requires 373.0374 and 375.0354.

4.1.3.3. 4-{[(4-Benzyl-5-methyl-1H-imidazol-2-yl)thio]methyl}benzoni-trile (2c).. Colorless crystals; yield 0.59 g (92%); mp 158–160 °C. [1]H

NMR (CDCl$_3$) ä [ppm]: 2,14 (s, 3H, CH$_3$), 3.82 (s, 2H, CH$_2$-C4), 4.04 (s, 2H, S-CH$_2$), 7.09–7.31 (m, 5H, H$_{arom}$ at C4), 7.15 (d, J = 8.0 Hz, 2H, H$_{arom}$ at *C2*), 7.40 (d, J = 8.0 Hz, 2H, H$_{arom}$ at *C2*), 8.55, 9.22 (2 s, 1H, NH, tautomeric). ^{13}C NMR (CDCl$_3$) [ä ppm]: 39.65 (S-CH$_2$), 110.95, 118.69 (CN), 126.71, 128.34, 128.65, 129.49, 132.20, 134.67, 143.81 (C$_{arom}$). HRMS-ESI: m/z = 320.1206 (C$_{19}$H$_{18}$N$_3$S, [M + H$^+$]); requires 320.1221.

4.1.3.4. 4-Benzyl-5-methyl-2-[(2,6-difluorobenzyl)thio]-1H-imidazole (2d).. Colorless crystals; yield 0.56 g (85%); mp 120–122 °C. ^{1}H NMR (CDCl$_3$) ä [ppm]: 2.14 (s, 3H, CH$_3$), 3.85 (s, 2H, CH$_2$-C4), 4.06 (s, 2H, S-CH$_2$), 6.73, 6.76 (t, J = 7.9 Hz, 2H, H$_{arom}$ at *C2*), 7.08–7.29 (m, 6H, H$_{arom}$ at *C2* and C4), 8.98 (s, 1H, NH). ^{13}C NMR (CDCl$_3$) [ä ppm]: 27.38 (S-CH$_2$), 111.00–111.14, 114.78, 126.27, 128.40, (C$_{arom}$), 128.90 (t, J_{CF} = 10.5 Hz, C`4, C$_{arom}$ at *C2*), 129.07, 134.94 (C$_{arom}$), 161.61 (dd, J_{CF} = 7.7, 249.8 Hz, C2′ & C6′, C$_{arom}$ at *C2*). HRMS-ESI: m/z = 331.1069 (C$_{18}$H$_{17}$F$_2$N$_2$S, [M + H$^+$]); requires 331.1081.

4.1.3.5. 4-Benzyl-2-[(4-methylbenzyl)thio]-5-methyl-1H-imidazole (2e).. Colourless crystals; yield 0.54 g (88%); mp 155–157 °C. ^{1}H NMR (DMSO-d_6) ä [ppm]: 2.06 (s, 3H, CH$_3$-C5), 2.25 (s, 3H, (p-CH$_3$-Bz), 3.32 (s, 2H, CH$_2$-C4), 4.11 (s, 2H, S-CH$_2$), 7.04 (d, J = 8.3 Hz, 2H, H$_{arom}$ at *C2*), 7.09 (d, J = 8.3 Hz, 2H, H$_{arom}$ at *C2*), 7.15–7.22 (m, 3H, H$_{arom}$ at C4), 7.27 (t, J = 8.3 Hz, 2H, H$_{arom}$ at C4) 11.82 (1H, NH). ^{13}C NMR (DMSO-d_6) [ä ppm]: 21.16 (p-CH$_3$-Bz), 38.18 (S-CH$_2$), 126.20, 128.67, 129.09, 129.34, 135.50, 136.64 (C$_{arom}$). HRMS-ESI: m/z = 309.1467 (C$_{19}$H$_{21}$N$_2$S, [M + H$^+$]); requires 309.1425.

4.1.4. 4-Benzyl-2-benzylsulfonyl-5-methyl-1H-imidazole (3).

A solution of **2a** (0.59 g, 2.0 mmol) in ethanol was treated with hydrogen peroxide (3.0 mL). The reaction mixture was heated at 60 °C for 24 h, and then cooled to rt. The solid was obtained by removal of the solvent followed by crystallization from ethanol to give **3** (0.45 g) as colorless crystals; yield 70%; mp 193–195 °C. IR (KBr) í [cm^{-1}]: 3085 (NH); 1636 (C=N); 1602, 1495 (C=C); 1319, 1121 (SO$_2$); 1070, 1111 (C—S—C). ^{1}H NMR (DMSO-d_6) ä [ppm]: 2.12 (s, 3H, CH$_3$), 3.87 (s, 2H, CH$_2$-C4), 4.68 (s, 2H, SO$_2$-CH$_2$), 7.07–7.31 (m, 10H, H$_{arom}$), 13.07, 13.17 (2 s, 1H, NH, tautomeric). ^{13}C NMR (DMSO-d_6) [ä ppm]: 9.55 (CH$_3$), 32.97 (CH$_2$-C4), 60.89 (SO$_2$-CH$_2$), 126.35, 126.37, 128.60, 128.77, 128.79, 128.87, 131.35, 136.65, 138.86, 139.49, 140.76 (C$_{arom}$, C5, C4 and *C2*). HRMS-ESI: m/z = 327.1146 (C$_{18}$H$_{19}$N$_2$O$_2$S, [M + H$^+$]); requires 327.1167.

4.1.5. 4-benzyl-5-methyl-2-[(2-nitrophenyl)thio]-1H-imidazole (4).

Under anhydrous conditions, a mixture of **1** (0.20 g, 1.0 mmol), 1-flouro-2-nitrobenzene (0.10 mL, 1.0 mmol) and sodium hydride (0.048 g, of a 55% suspension in paraffin oil, 2.0 mmol) in dimethylformamide (5.0 mL) was stirred for 12 h at rt. The reaction mixture was treated with ice-cold water (100 mL) and left to stand at rt for 3 h. The solid product was isolated by filtration and crystallized from ethanol to give **4** (0.26 g) as pale orange crystals; yield 80%; mp 181–182 °C. ^{1}H NMR (DMSO-d_6) ä [ppm]: 2.18 (s, 3H, CH$_3$), 3.89 (s, 2H, CH$_2$-C4), 6.77 (d, J = 7.6 Hz, 1H, H$_{arom}$ at *C2*), 7.21–7.30 (m, 5H, H$_{arom}$ at C4), 7.43 (t, J = 7.6 Hz, 1H, H$_{arom}$ at *C2*), 7.63 (t, J = 7.6 Hz, 1H, H$_{arom}$ at *C2*), 8.25 (d, J = 7.6 Hz, 1H, H$_{arom}$ at *C2*), 12.68 (s, 1H, NH). ^{13}C NMR (DMSO-d_6) [ä ppm]: 9.81, 12.93 (CH$_3$, tautomeric), 31.15, 33.03 (CH$_2$-C4, tautomeric) 126.29, 126.90, 128.26, 128.71, 130.26, 135.10, 137.75, 139.94, 141.08 and 144.83 (C$_{arom}$, C5, C4 and *C2*). HRMS-ESI: m/z = 326.0952 (C$_{17}$H$_{15}$N$_3$O$_2$S, [M + H$^+$]); requires 326.0963.

4.1.6. 4-Benzyl-2-[(2,4-dinitrophenyl)thio]-5-methyl-1H-imidazole (5).

To a solution of potassium hydroxide (0.056 g, 1.0 mmol) in methanol (15 mL), **1** (0.20 g, 1.0 mmol) was added and the mixture was stirred for 0.5 h. 1-chloro-2,4-dinitrobenzene (0.20 g, 1.0 mmol) was added to the reaction mixture and stirred at rt for an additional 6 h. The

solvent was removed under reduced pressure, water (25 mL) was added to the residual material. The solid product was filtered off and recrystallized from ethanol to give 0.315 g of compounds **5** as yellow-orange crystals; yield 85%; mp 105–106 °C. ^{1}H NMR (DMSO-d_6) ä [ppm]: 2.20 (s, 3H, CH$_3$), 3.91 (s, 2H, CH$_2$-C4), 6.97 (d, J = 9.0 Hz, 1H, H$_{arom}$ at *C2*), 7.17–7.33 (m, 5H, H$_{arom}$ at C4), 8.43 (dd, J = 2.6, 9.0 Hz. 1H, H$_{arom}$ at *C2*), 8.99 (d, J = 2.6 Hz, 1H, H$_{arom}$ at *C2*), 12.68 (s, 1H, NH). ^{13}C NMR (DMSO-d_6) [ä ppm]: 9.84 (CH$_3$), 33.10 (CH$_2$-C4), 121.82, 126.22, 128.63, 128.76, 129.41, 140.56, 141.06, 144.05, 145.24, 146.07 (C$_{arom}$, C5, C4 and *C2*). HRMS-ESI: m/z = 371.0727 (C$_{17}$H$_{14}$N$_4$O$_4$S, [M + H$^+$]); requires 371.0814.

4.1.7. 2-Aroylmethylthio-4-benzyl-5-methyl-1H-imidazoles (6a, b).

Under anhydrous conditions, a mixture of **1** (0.20 g, 1 mmol), the appropriate phenacyl bromide derivatives (1.0 mmol) and sodium hydride (0.048 g, of a 55% suspension in paraffin oil, 2.0 mmol) in dimethylformamide (5.0 mL) was stirred for 2 h at rt. The reaction mixture was treated with ice-cold water (100 mL) and left to stand at rt for 3 h. The solid product was isolated by filtration and recrystallized from acetone/water to give compounds **6a,b**.

4.1.7.1. 4-Benzyl-2-benzoylmethylthio-5-methyl-1H-imidazole (6a).. Colorless crystals; yield 0.95 g (92%); mp 156–157 °C. ^{1}H NMR (CDCl$_3$) ä [ppm]: 2.15 (s, 3H, CH$_3$), 3.85 (s, 2H, CH$_2$-C4), 4.31 (s, 2H, S-CH$_2$), 7.15–7.29 (m, 5H, H$_{arom}$ at C4), 7.44 (t, J = 7.4 Hz, 2H, H$_{arom}$ at *C2*), 7.58 (t, J = 7.4 Hz, 1H, H$_{arom}$ at *C2*), 7.90 (d, J = 7.4 Hz, 2H, H$_{arom}$ at *C2*). ^{13}C NMR (CDCl$_3$) [ä ppm]: 41.33 (S-CH$_2$), 126.28, 128.41, 128.55, 128.62, 128.80, 133.89, 135.31 (C$_{arom}$). HRMS-ESI: m/z = 323.1190 (C$_{19}$H$_{19}$N$_2$OS, [M + H$^+$]); requires 323.1218.

4.1.7.2. 4-Benzyl-2-(4-chlorobenzoylmethylthio)-5-methyl-1H-imidazole (6b).. Colourless crystals; yield 0.31 g (87%); mp 165–168 °C. ^{1}H NMR (DMSO-d_6) ä [ppm]: 2.04 (s, 3H, CH$_3$), 3.72 (s, 2H, CH$_2$-C4), 4.53 (s, 2H, S-CH$_2$), 7.14–7.27 (m, 5H, H$_{arom}$ at C4), 7.55 (d, J = 8.5 Hz, 2H, H$_{arom}$ at *C2*), 7.93 (d, J = 8.5 Hz, 2H, H$_{arom}$ at *C2*), 11.89 (s, 1H, NH). ^{13}C NMR (DMSO-d_6) [ä ppm]: 128.64, 128.67, 129.21, f130.85, 134.55, 136.19, 138.79 (C$_{arom}$), 193.94 (C=O). HRMS-ESI: m/z = 357.0812 and 359.0790 (C$_{19}$H$_{18}^{35}$ClN$_2$OS, C$_{19}$H$_{18}^{37}$ClN$_2$OS [M + H$^+$]); requires 357.0828 and 358.0799.

4.1.8. 2-[(4-Benzyl-5-methyl-1H-imidazol-2-yl)thio]-N-(aryl)acetamides (7a-h).

Under anhydrous condition, compound **1** (0.204 g, 1 mmol) was dissolved in dimethylformamide (5 mL), sodium hydride (0.048 g, of its 55% suspension in paraffin oil, 2 mmol) was added to the solution portion-wise under ice cooling. After stirring the mixture for 0.5 h, appropriate chloroacetanilide derivatives (1 mmol) was added portion-wise to the reaction mixture under ice cooling stirred at rt for 4 h. The reaction mixture was treated with ice/cold water (100 mL) and left to stand at rt for 3 h. The solid product was isolated by filtration and recrystallized from ethanol/water to give compounds **7a-h**.

4.1.8.1. 2-[(4-Benzyl-5-methyl-1H-imidazol-2-yl)thio]-N-phenyl-acetamide (7a).. Colorless crystals; yield 0.315 g (93%); mp 156–157 °C. ^{1}H NMR (DMSO-d_6) ä [ppm]: 2.09, 2.12 (2 s, 3H, CH$_3$, tautomeric), 3.77 (s, 2H, CH$_2$-C4), 3.81, 3.84 (2 s, 2H, S-CH$_2$, tautomeric), 7.02–7.60 (m, 10H, H$_{arom}$.), 10.57, 10.62 (2 s, 1H, NHCO, tautomeric), 12.04 (s, 1H, NH of N1). ^{13}C NMR (DMSO-d_6) [ä ppm]: 9.66 (CH$_3$), 32.99 (CH$_2$-C4), 38.53 (S-CH$_2$), 119.45, 123.84, 126.11, 128.64, 128.80, 129.23, 134.38, 136.98, 137.07, 139.40, 141.44 (C$_{arom}$, C5, C4 and *C2*), 167.51 (C=O). HRMS-ESI: m/z = 338.1303 (C$_{19}$H$_{20}$N$_3$OS, [M + H$^+$]); requires 338.1327.

4.1.8.2. 2-[(4-Benzyl-5-methyl-1H-imidazol-2-yl)thio]-N-(4-chlor-ophenyl)acetamide (7b).. Colourless crystals; yield 0.34 g (92%); mp

199–202 °C. ^{1}H NMR (DMSO-d_6) ä [ppm]: 2.10 (s, 3H, CH$_3$), 3.79 (s, 2H, CH$_2$-C4), 3.82 (s, 2H, S-CH$_2$), 7.16–7.24 (m, 5H, H$_{arom}$ at C4), 7.33 (d, J = 8.4 Hz, 2H, H$_{arom}$ at C2), 7.51–7.53 (m, 2H, H$_{arom}$ at C2), 10.73 (s, 1H, NHCO), 12.06 (s, 1H, NH of N1). ^{13}C NMR (DMSO-d_6) [ä ppm]: 10.39 (CH$_3$), 32.75 (CH$_2$-C4), 38.51 (S-CH$_2$), 121.00, 126.25, 126.34, 127.39, 128.72, 129.15, 136.09, 138.36 (C$_{arom}$), 167.65 (C=O). HRMS-ESI: m/z = 372.0915 and 374.0894 (C$_{19}$H$_{19}$N$_3$OS^{35}Cl, C$_{19}$H$_{19}$N$_3$OS^{37}Cl [M + H$^+$]); requires 372.0937 and 374.0908.

4.1.8.3. 2-[(4-Benzyl-5-methyl-1H-imidazol-2-yl)thio]-N-(3-chlorophenyl)acetamide (7c).

Colorless crystals; yield 0.33 g (90%); mp 135–137 °C. ^{1}H NMR (DMSO-d_6) ä [ppm]: 2.09 (s, 3H, CH$_3$), 3.77 (s, 2H, CH$_2$-C4), 3.80 (s, 2H, S-CH$_2$), 7.09–7.21 (m, 6H, H$_{arom}$ at C4 and C2), 7.31 (d, J = 5.3 Hz, 2H, H$_{arom}$ at C4), 7.80 (s, 1H, H$_{arom}$ at C2). ^{13}C NMR (DMSO-d_6) [ä ppm]: 11.03 (CH$_3$), 31.99 (CH$_2$-C4), 38.57 (S-CH$_2$), 117.84, 118.97, 123.48, 126.20, 128.68, 130.92, 133.57, 136.20, 140.97 (C$_{arom}$), 168.08 (C=O). Anal. calcd. for C$_{19}$H$_{18}$ClN$_3$OS (371.08): C, 61.36; H, 4.88; Cl, 9.53; N, 11.30; S, 8.62. Found: C, 61.02; H, 5.06; Cl, 9.30; N, 11.50; S, 8.69%.

4.1.8.4. 2-[(4-Benzyl-5-methyl-1H-imidazol-2-yl)thio]-N-(p-tolyl)acetamide (7d).

Colorless crystals; yield 0.32 g (91%); mp 211–212 °C. ^{1}H NMR (DMSO-d_6) ä [ppm]: 2.11 (s, 3H, CH$_3$), 2.25 (s, 3H, CH_3-Ph), 3.79 (s, 4H, CH$_2$-C4 and S-CH$_2$), 7.09 (t, J = 7.7 Hz, 2H, H$_{arom}$ at C4), 7.17–7.23 (m, 5H, H$_{arom}$ at C4 and C2), 7.35 (d, J = 7.9 Hz, 1H, H$_{arom}$ at C2), 7.45 (d, J = 7.0 Hz, 1H, H$_{arom}$ at C2), 10.47, 10.51 (2 s, 1H, NHCO, tautomeric), 12.03 (s, 1H, NH of N1). ^{13}C NMR (DMSO-d_6) [ä ppm]: 9.67 (CH$_3$), 20.92 (CH_3-Ph), 33.01 (CH$_2$-C4), 38.50 (S-CH$_2$), 119.46, 126.13, 128.64, 128.80, 129.61, 132.78, 136.63, 136.91, 137.08, 141.45 (C$_{arom}$, C5, C4 and C2), 167.21 (C=O). HRMS-ESI: m/z = 352.1448 (C$_{20}$H$_{22}$N$_3$OS, [M + H$^+$]); requires 352.1484.

4.1.8.5. 2-[(4-Benzyl-5-methyl-1H-imidazol-2-yl)thio]-N-(m-tolyl)acetamide (7e).

Colorless crystals; yield 0.315 g (90%); mp 145–147 °C. ^{1}H NMR (DMSO-d_6) ä [ppm]: 2.09 (s, 3H, CH$_3$), 2.25 (s, 3H, CH_3-Ph), 3.80 (s, 4H, CH$_2$-C4 and S-CH$_2$), 6.88 (d, J = 7.1 Hz, 1H, H$_{arom}$ at C2), 7.14–7.39 (m, 8H, H$_{arom}$.), 10.47, 10.54 (2 s, 1H, NHCO, tautomeric), 12.01 (s, 1H, NH of N1). ^{13}C NMR (DMSO-d_6) [ä ppm]: 12.78 (CH$_3$), 21.64 (CH_3-Ph), 32.99 (CH$_2$-C4), 38.55 (S-CH$_2$), 116.69, 119.99, 124.25, 126.08, 128.61, 128.77, 129.09, 135.57, 138.42, 139.34 (C$_{arom}$), 167.38 (C=O). HRMS-ESI: m/z = 352.1477 (C$_{20}$H$_{22}$N$_3$OS, [M + H$^+$]); requires 352.1484.

4.1.8.6. 2-[(4-Benzyl-5-methyl-1H-imidazol-2-yl)thio]-N-(4-methoxyphenyl)acetamide (7f).

Colorless crystals; yield 0.31 g (85%); mp 199–202 °C. ^{1}H NMR (DMSO-d_6) ä [ppm]: 2.11 (s, 3H, CH$_3$), 3.72 (s, 3H, CH$_3$-O), 3.78 (s, 4H, CH$_2$-C4 and S-CH$_2$), 6.88 (t, J = 7.9 Hz, 2H, H$_{arom}$ at C4), 7.17–7.23 (m, 5H, H$_{arom}$ at C4 and C2), 7.38 (d, J = 8.44 Hz, 1H, H$_{arom}$ at C2), 7.48 (d, J = 5.87 Hz, 1H, H$_{arom}$ at C2), 10.40, 10.43 (2 s, 1H, NHCO, tautomeric), 12.03 (s, 1H, NH of N1). ^{13}C NMR (DMSO-d_6) [ä ppm]: 9.65 (CH$_3$), 32.98 (CH$_2$-C4), 38.45 (S-CH$_2$), 55.64 (CH$_3$-O), 114.37, 120.98, 126.11, 128.66, 128.79, 132.58, 155.76 (C$_{arom}$), 166.93 (C=O). HRMS-ESI: m/z = 368.1402 (C$_{20}$H$_{22}$N$_3$O$_2$S, [M + H$^+$]); requires 368.1433.

4.1.8.7. 2-[(4-Benzyl-5-methyl-1H-imidazol-2-yl)thio]-N-(4-cyanophenyl)acetamide (7 g).

Colorless crystals; yield 0.34 g (94%); mp 190–191 °C. ^{1}H NMR (DMSO-d_6) ä [ppm]: 2.10 (s, 3H, CH$_3$), 3.77 (s, 2H, CH$_2$-C4), 3.86 (s, 2H, S-CH$_2$), 7.15–7.20 (m, 5H, H$_{arom}$ at C4), 7.65–7.75 (m, 4H, H$_{arom}$ at C2), 11.03 (s, 1H, NHCO), 12.06 (s, 1H, NH of N1). ^{13}C NMR (DMSO-d_6) [ä ppm]: 9.60 (CH$_3$), 32.91 (CH$_2$-C4), 38.60 (S-CH$_2$), 105.52 (C$_{arom}$), 119.48 (CN), 124.62, 126.06, 128.69, 128.73, 133.79, 135.93, 143.58 (C$_{arom}$), 168.35 (C=O). HRMS-ESI: m/z = 363.1256 (C$_{20}$H$_{19}$N$_4$OS, [M + H$^+$]); requires 363.1280.

4.1.8.8. 2-[(4-Benzyl-5-methyl-1H-imidazol-2-yl)thio]-N-(4-bromophenyl)acetamide (7 h).

Colorless crystals; yield 0.39 g (94%); mp 205–207 °C. ^{1}H NMR (DMSO-d_6) ä [ppm]: 2.09 (s, 3H, CH$_3$), 3.78 (s, 2H, CH$_2$-C4), 3.81 (s, 2H, S-CH$_2$), 7.15–7.23 (m, 5H, H$_{arom}$ at C4), 7.42–7.47 (m, 4H, H$_{arom}$ at C2), 10.71 (s, 1H, NHCO), 12.03 (s, 1H, NH of N1). ^{13}C NMR (DMSO-d_6) [ä ppm]: 38.38 (S-CH$_2$), 115.38, 121.36, 126.28, 128.70, 128.71, 132.04, 136.06, 138.76 (C$_{arom}$), 167.65 (C=O). Anal. calcd. For C$_{19}$H$_{18}$BrN$_3$OS (415.03): C, 54.81; H, 4.36; Br, 19.19; N, 10.09; S, 7.70. Found: C, 54.74; H, 4.52; Br, 19.02; N, 10.25; S, 7.57%

4.1.9. Ethyl 2-[(4-Benzyl-5-methyl-1H-imidazol-2-yl)thio]acetate (8).

To a stirred solution of **1** (4.08 g, 20.0 mmol) in acetone (100 mL) was added potassium carbonate (2.76 g, 20.0 mmol) and the reaction mixture was stirred at rt for 1 h. Ethyl chloroacetate (2.15 mL, 20.0 mmol) was added dropwise to the reaction mixture and stirred for additional 6 h at rt. The solvent was removed under reduced pressure and the residue was treated with water (20 mL), filtered off and crystallized from ethanol/water to afford 4.6 g of compound **8** as colorless crystals; yield 80%; mp 155–156 °C. ^{1}H NMR (CDCl$_3$) ä [ppm]: 1.21, 1.27 (2 t, J = 7.4 Hz, 3H, CH$_2$CH_3, tautomeric), 2.13, 2.19 (2 s, 3H, CH$_3$-C5, tautomeric), 3.56 (s, 3H, CH$_2$-C4), 3.85, 3.88 (2 s, 2H, S-CH$_2$, tautomeric), 4.13, 4.21 (2q, J = 7.4 Hz, 2H, CH_2CH$_3$), 7.15 (m, 1H, H$_{arom}$ at C4), 7.22–7.30 (m, 4H, H$_{arom}$ at C4), 9.69, 9.92 (2 s, 1H, NH, tautomeric). ^{13}C NMR (CDCl$_3$) [ä ppm]: 9.78, 11.37 (CH$_3$, at C5), 12.47, 14.03 (CH$_2$CH$_3$), 30.70 (CH$_2$-C4), 33.46, 36.71 (S-CH$_2$), 61.98, 62.09 (CH$_2$CH$_3$), 125.84, 126.68, 128.29, 128.32, 128.51, 128.78, 130.65, 130.79, 134.80, 135.49, 137.95, 138.48, 140.60, 141.35 (C$_{arom}$, C5, C4 and C2), 171.60 (C=O). HRMS-ESI: m/z = 291.1165 (C$_{15}$H$_{19}$N$_2$O$_2$S, [M + H$^+$]); requires 291.1167. Anal. calcd. for C$_{15}$H$_{18}$N$_2$O$_2$S (290.10): C, 62.04; H, 6.25; N, 9.65; S, 11.04. Found: C62.22; H, 610; N, 9.81; S, 10.96%.

4.1.10. 2-[(4-Benzyl-5-methyl-1H-imidazol-2-yl)thio]-N-(2-(dimethylamino)ethyl-acetamide (9).

A mixture of **8** (0.58 g, 2.0 mmol) and *N,N*-dimethylethylenediamine (3.0 mL, 10 mmol) in 1,4-dioxane (25 mL) was heated under reflux for 36 h. The solvent was evaporated under reduced pressure. The residue was treated with water, filtered off, recrystallized from ethanol to afford **9** as colorless crystals; yield 0.33 g (50%); mp 165–166 °C. ^{1}H NMR (CDCl$_3$) ä [ppm]: 2.07 (s, 3H, CH$_3$-C5), 2.10 (s, 6H, 2CH$_3$, N(CH$_3$)$_2$), 2.22 (t, J = 6.6, 2H, NHCH$_2$CH_2N(CH$_3$)$_2$), 3.11 (q, J = 6.6, 2H, NHCH_2CH$_2$N(CH$_3$)$_2$), 3.32 (s, 2H, CH$_2$-C4), 3.75 (s, 2H, S-CH$_2$), 7.13–7.20 (m, 3H, H'2, H'4 & H'6, H$_{arom}$ at C4), 7.21–7.28 (m, 2H, H'3 & H'5, H$_{arom}$), 8.17 (s, 1H, NHCO), 11.90 (s, 1H, NH of N1). ^{13}C NMR (CDCl$_3$) [ä ppm]: 10.21 (CH$_3$), 37.34 (CH$_2$-C4), 37.51(S-CH$_2$), 45.58, 58.40 (2CH$_3$, N-(CH$_3$)$_2$), 126.22, 128.70 (C$_{arom}$), 168.41 (C=O). HRMS-ESI: m/z = 333.1740 (C$_{17}$H$_{25}$N$_4$OS, [M + H$^+$]); requires 333.1749.

4.1.11. 2-[(4-Benzyl-5-methyl-1H-imidazol-2-yl)thio]-N,N-dimethylacetamide (10a).

As described for **9**, using dimethylamine (10 mL), the reaction mixture was heated under reflux for 24 h to give **10a** (0.35 g) as colourless crystals; yield 60%; mp 168–170 °C. ^{1}H NMR (CDCl$_3$) ä [ppm]: 2.17 (s, 3H, CH$_3$), 2.99, 3.03 (2 s, 6H, 2CH$_3$, N(CH$_3$)$_2$), 3.68 (s, 2H, CH$_2$-C4), 3.87 (s, 2H, S-CH$_2$), 7.16–7.30 (m, 5H, H$_{arom}$). ^{13}C NMR (CDCl$_3$) [ä ppm]: 10.95 (CH$_3$), 32.22 (CH$_2$-C4), 35.01(S-CH$_2$), 36.23, 37.89 (2CH$_3$, N(CH$_3$)$_2$), 126.07, 128.40, 128.43, 136.23 (C$_{arom}$), 170.12 (C=O). Anal. calcd. for C$_{15}$H$_{19}$N$_3$OS (289.10): C, 62.25; H, 6.62; N, 14.52; S, 11.08. Found: C, 62.5; H, 6.6; N, 14.3; S, 11.0%.

4.1.12. 2-[(4-Benzyl-5-methyl-1H-imidazol-2-yl)thio]-N-cyclohexylacetamide (10b).

As described for **9** using cyclohexylamine (5.0 mL), the reaction mixture was heated under reflux for 48 h to give **10b** (0.36 g) as colorless crystals; yield 53%; mp 166–168 °C. ^{1}H NMR (CDCl$_3$) ä [ppm]: 1.06–1.83 (m, 10H, 5CH$_2$, C$_6$H$_{11}$), 2.18 (s, 3H, CH$_3$), 3.44 (s, 2H, CH$_2$-

C4), 3.68–3.72 (m, 1H, CH, cC$_6$H$_{11}$), 3.84 (s, 2H, S-CH$_2$), 7.14–7.30 (m, 5H, H$_{arom}$), 7.86, 7.88 (s, 1H, NHCO, tautomeric). ^{13}C NMR (CDCl$_3$) [ä ppm]: 9.40 (CH$_3$), 23.96, 24.61, 25.47, 30.36 (cC$_6$H$_{11}$), 32.43 (CH$_2$-C4), 37.27 (S-CH$_2$), 48.73 (cC$_6$H$_{11}$), 126.21, 128.39, 128.49, 136.99 (C$_{arom}$), 169.33 (C=O). Anal. calcd. for C$_{19}$H$_{25}$N$_3$OS (343.17): C, 66.44; H,7.34; N, 12.23; S, 9.34. Found: C, 66.2; H, 7.50; N, 12.4; S, 9.51%.

4.1.13. 2-[(4-Benzyl-5-methyl-1H-imidazol-2-yl)thio]acetohydrazide (11).

A mixture of **8** (5.80 g, 20.0 mmol) and hydrazine hydrate (10 mL) was heated in ethanol (100 mL) at 60 °C for 6 h. The solvent was evaporated under reduced pressure. The residue was treated with water, filtered off, crystallized from ethanol to afford **11** (3.3 g) as colorless crystals; yield 60%; mp 180–184 °C. ^{1}H NMR (DMSO-d_6) ä [ppm]: 2.08 (s, 3H, CH$_3$), 3.58 (s, 2H, CH$_2$-C4), 3.74 (s, 2H, S-CH$_2$), 4.28 (s, 2H, NHN*H*$_2$), 7.18–7.26 (m, 5H, H$_{arom}$ at C4), 9.35 (s, H, CON*H*NH$_2$), 11.93 (s, 1H, NH of N1). ^{13}C NMR (DMSO-d_6) [ä ppm]: 9.75 (CH$_3$), 31.58 (CH$_2$-C4), 34.06 (S-CH$_2$), 126.62, 128.70, 128.81 (C$_{arom}$), 167.83 (C=O). Anal. calcd. for C$_{13}$H$_{16}$N$_4$O4S (276.10): C, 56.50; H, 5.84; N, 20.27; S, 11.60. Found: C, 56.4; H, 6.04; N, 20.1; S, 11.8%.

4.1.14. 2-[(4-Benzyl-5-methyl-1H-imidazol-2-yl)thio]-N'-arylideneacetohydrazides (12a-e).

To a solution of **11** (0.55 g, 2.0 mmol) in ethanol (25 mL), appropriate aromatic aldehyde (2.0 mmol) and 2 drops of glacial acetic acid were added. The reaction mixture was stirred for 6 h with **12a or 12b**; for 12 h with **12c** and for 24 h with **12d** or **12e**) at rt. The solid formed was filtered, washed with water, and crystallized from ethanol to afford products **12a-e.**

4.1.14.1. 2-[(4-Benzyl-5-methyl-1H-imidazol-2-yl)thio]-N'-benzylideneacetohydrazide (12a).

Colorless crystals; yield 0.64 g (88%); mp 194–195 °C. ^{1}H NMR (DMSO-d_6) ä [ppm]: 2.01, 2.10 (2 s, 3H, CH$_3$, tautomeric), 3.68, 3.75, (2 s, 2H, CH$_2$-C4, tautomeric), 3.78, 4.14 (2 s, 2H, S-CH$_2$, tautomeric), 7.15–7.26 (m, 5H, H$_{arom}$ at C4), 7.42–7.46 (m, 3H, H'3, H'4 & H'5, H$_{arom}$ at C2), 7.64–7.67 (m, 2H, H'2 & H'6, H$_{arom}$ at C2), 7.96 (s, 1H, N = CH), 11.50, 11.87 (2 s, 1H, NH = N, tautomeric), 11.95, 12.03 (2 s, 1H, NH of N1, tautomeric). ^{13}C NMR (DMSO-d_6) [ä ppm]: 9.63 (CH$_3$), 35.71 (CH$_2$-C4), 35.89 (S-CH$_2$), 127.30, 127.57, 128.55, 128.82, 129.23, 129.27, 130.31, 130.58, 132.51, 134.55 (C$_{arom}$), 143.67, 147.22 (N = CH). 160.61, 161.62 (C=O). Anal. calcd. for C$_{20}$H$_{20}$N$_4$OS (364.13): C, 65.91; H, 5.53; N, 15.37; S, 8.80. Found: C, 66.2; H, 5.67; N, 15.2; S, 8.64%.

4.1.14.2. 2-[(4-Benzyl-5-methyl-1H-imidazol-2-yl)thio]-N'-(4-chlorobenzylidene)aceto-hydrazide (12b).

Colorless crystals; yield 0.66 g (83%); mp 189–190 °C. ^{1}H NMR (DMSO-d_6) ä [ppm]: 1.99, 2.09 (2 s, 3H, CH$_3$, tautomeric), 3.66, 3.74 (2 s, 2H, CH$_2$-C4, tautomeric), 4.08, 4.12 (s, 2H, S-CH$_2$, tautomeric), 7.11–7.23 (m, 5H, H$_{arom}$ at C4), 7.50–7.69 (m, 4H, H$_{arom}$ at C2) 7.89, 7.92 (2 s, 1H,N = CH, tautomeric), 11.54, 11.92 (2 s, 1H, NH = N, tautomeric), 11.92, 12.01 (2 s, 1H, NH of N1, tautomeric). ^{13}C NMR (DMSO-d_6) [ä ppm]: 8.51 (CH$_3$), 35.71 (CH$_2$-C4), 38.09 (S-CH$_2$), 124.61, 128.54, 128.79, 128.91, 129.28, 129.58, 130.50, 133.51, 134.99 (C$_{arom}$) 145.90, 146.33 (N = CH), 161.07 (C=O). Anal. calcd. for C$_{20}$H$_{19}$ClN$_4$OS (398.09): C, 60.22; H, 4.80; Cl, 8.89; N, 14.05; S, 8.04. Found: C, 59.9; H, 4.58; Cl, 8.78; N, 13.9; S, 8.25%.

4.1.14.3. 2-[(4-Benzyl-5-methyl-1H-imidazol-2-yl)thio]-N'-(4-bromobenzylidene)aceto-hydrazide (12c).

Colorless crystals; yield 0.70 g (80%); mp 180–182 °C. ^{1}H NMR (DMSO-d_6) ä [ppm]: 2.00, 2.09 (2 s, 3H, CH$_3$, tautomeric), 3.72 (s, 2H, CH$_2$-C4), 4.30 (s, 2H, S-CH$_2$), 7.17–7.22 (m, 5H, H$_{arom}$ at C4), 7.59–7.75 (m, 4H, H$_{arom}$ at C2), 7.92 (s, 1H, N = CH), 11.55 (s, 1H, NH = N), 11.92, 12.01 (2 s, 1H, NH of N1, tautomeric). ^{13}C NMR (DMSO-d_6) [ä ppm]: 123.46, 123.79, 127.96, 128.54, 128.81, 129.14, 130.68, 132.80, 132.71, 133.83 (C$_{arom}$),

142.46, 146.90 (N = CH), 170.42 (C=O). Anal. calcd. for C$_{20}$H$_{19}$BrN$_4$OS (442.04) C, 54.18; H, 4.32; Br, 18.02; N, 12.64 S, 7.23. Found: C, 54.4; H, 4.46; Br, 17.9; N, 12.7; S, 7.36%.

4.1.14.4. 2-[(4-Benzyl-5-methyl-1H-imidazol-2-yl)thio]-N'-(4-methoxybenzylidene)aceto-hydrazide (12d).

Colorless crystals; yield 0.63 g (80%); mp 192–194 °C. ^{1}H NMR (DMSO-d_6) ä [ppm]: 2.09, 2.10 (2 s, 3H, CH$_3$, tautomeric), 3.71 (s, 2H, CH$_2$-C4), 3.79 (s, OCH$_3$), 4.09 (s, 2H, S-CH$_2$), 6.95–7.00 (m, 2H, H$_{arom}$ at C2), 7.11–7.23 (m, 5H, H$_{arom}$ at C4), 7.55–7.59 (m, 2H, H$_{arom}$ at C2), 7.90 (s, 1H, N = CH), 11.36, 11.719 (2 s, 1H, NH = N), 11.92, 12.01 (2 s, 1H, NH of N1, tautomeric). ^{13}C NMR (DMSO-d_6) [ä ppm]: 55.77 (O-CH$_3$), 114.70, 114.76, 127.15, 128.60, 128.87, 129.16 (C$_{arom}$), 143.57, 147.11, (N = CH), 161.09, 161.32 (C$_{arom}$), 170.05 (C=O). Anal. calcd. for C$_{21}$H$_{22}$N$_4$O$_2$S (394.14): C, 63.94; H, 5.62; N, 14.20; S, 8.13. Found: C, 64.2; H, 5.82; N, 14.5; S, 8.36%.

4.1.14.5. 2-[(4-Benzyl-5-methyl-1H-imidazol-2-yl)thio]-N'-(2,4-dimethoxybenzylidene)-acetohydrazide (12e).

Colorless crystals; yield 0.65 g (79%); mp 170–171 °C. ^{1}H NMR (DMSO-d_6) ä [ppm]: 2.00, 2.09 (2 s, 3H, CH$_3$, tautomeric), 3.72 (s, 2H, CH$_2$-C4), 3.79, 3.83 (2 s, 6H, 2 (OCH$_3$), 4.12 (s, 2H, S-CH$_2$), 7.00 (t, J = 9.1 Hz, 1H, H$_{arom}$ at C4), 7.15–7.40 (m, 7H, H$_{arom}$ at C4 and C2), 7.78, 8.00 (2 s, 1H, N = CH), 11.40, 11.71 (2 s, 1H, NH = N), 11.92,11.99 (s, 1H, NH of N1, tautomeric). ^{13}C NMR (DMSO-d_6) [ä ppm]: 8.99 (CH$_3$), 36.55 (S-CH$_2$), 55,91, 56.04 (2(O-CH$_3$), 108.77, 109.01, 111.92, 127.22, 127.33, 128.69, 128.70, 134.08, 149.43 (N = CH), 151.21, 164.81 (C$_{arom}$), 171.07 (C=O). Anal. calcd. for C$_{22}$H$_{24}$N$_4$O$_3$S (424.15): C, 62.24; H, 5.70; N, 13.20; S, 7.50. Found: C, 62.4; H, 5.58; N, 13.3; S, 7.33%.

4.1.15. 2-[(4-Benzyl-5-methyl-1H-imidazol-2-yl)thio]-N'-(1-arylethylidene)acetohydrazide (12f, g).

To a solution of **11** (0.55 g, 2.0 mmol) in ethanol (25 mL), the appropriate aromatic ketones (2.0 mmol) and 2 drops of glacial acetic acid were added. The reaction mixture was stirred for 12 h (**12f**) or for 24 h (**12 g**) hours at rt. The solid formed was filtered, washed with water, crystallized from ethanol to afford compounds **12f** or **12 g.**

4.1.15.1. 2-[(4-Benzyl-5-methyl-1H-imidazol-2-yl)thio]-N'-(1-phenylethylidene)aceto-hydrazide (12f).

Colorless crystals; yield 0.67 g (89%); mp 164–166 °C. ^{1}H NMR (DMSO-d_6) ä [ppm]: 2.00, 2.10 (2 s, 3H, CH$_3$-C5, tautomeric), 2.23 (s, 3H, N=C(CH$_3$), 3.33 (2 s, 2H, CH$_2$-C4), 4.16 (s, 2H, S-CH$_2$), 7.14–7.25 (m, 5H, H$_{arom}$ at C4), 7.38–7.41 (m, 3H, H$_{arom}$ at C2), 7.75–7.77 (m, 2H, H$_{arom}$ at C2), 10.71, 11.00 (2 s, 1H, NH = N), 11.94, 12.09 (2 s, 1H, NH of N1, tautomeric). ^{13}C NMR (DMSO-d_6) [ä ppm]: 14.12 (N=C(CH$_3$), 126.56, 126.79, 128.78, 129.53, 129.75, 130.61, 138.46 (C$_{arom}$), 148.27 (N = CH), 171.15 (C=O). HRMS-ESI: m/z = 379.1547 (C$_{21}$H$_{23}$N$_4$OS, [M + H$^+$]); requires 379.1593.

4.1.15.2. 2-[(4-Benzyl-5-methyl-1H-imidazol-2-yl)thio]-N'-[1-(4-bromophenyl)ethylidene] acetohydrazide (12 g).

Colorless crystals; yield 0.81 g (89%); mp 177–179 °C. ^{1}H NMR (DMSO-d_6) ä [ppm]: 2.00, 2.10 (2 s, 3H, CH$_3$-C5, tautomeric), 2.21, 2.27 (s, 3H, N=C(CH$_3$), tautomeric), 3.78, 380 (2 s, 2H, CH$_2$-C4), 4.13 (s, 2H, S-CH$_2$), 7.14–7.25 (m, 5H, H$_{arom}$ at C4), 7.56–7.88 (m,4H, H$_{arom}$ at C2), 10.77, 11.06, 11.35 (3 s, 1H, NH = N), 11.94, 12.09 (2 s, 1H, NH of N1, tautomeric). ^{13}C NMR (DMSO-d_6) [ä ppm]: 15.12 (N=C(CH$_3$), 125.42, 126.93, 128.55, 128.80, 129.04, 131.71, 131.73, 132.71 (C$_{arom}$), 140.49, 145.46 (N = CH), 160.20 (C=O). HRMS-ESI: m/z = 457.0733 and 459.0715 (C$_{21}$H$_{22}$^{79}BrN$_4$OS, C$_{21}$H$_{22}$^{81}BrN$_4$OS [M + H$^+$]); requires 457.0698 and 459.0677.

4.2. Biological activity

4.2.1. Cells and reagents

All tested imidazole derivatives were dissolved in DMSO to form 100 μM stock solutions and were stored at −20 °C. Murine 4 T1-Luc2, and human MDA-MB-231 breast cancer cells, were maintained in Roswell Park Memorial Institute (RPMI)-1640 medium (Nissui, Tokyo, Japan) supplemented with 10% bovine serum and 20 U/mL penicillin, and 20 ìg/mL streptomycin, and the cells incubated at 37 °C in a humidified incubator in an atmosphere containing 5% CO_2 in the air. The primary antibodies against STAT3, p-STAT3, STAT1, and p-STAT1 were purchased from Cell Signaling Technology (Beverly, MA, USA) and the antibody against â-actin was purchased from Santa Cruz Biotechnology (Santa Cruz, CA, USA).

4.2.2. In vitro cell viability assay

The anti-tumor activity of tested compounds was quantified using WST-8 assay (Wako Pure Chemical Industries, Tokyo, Japan). The cells in the exponential growth were placed at a final concentration (10^4 cells/well) in a 96-well plate. After 24 h of incubation, the target compounds were added. Controls received DMSO vehicle at a concentration equal to that in drug-treated cells. After the incubation with test compounds for 72 h, WST-8 reagent was added and the absorbance at 450 nm/620 nm was measured using a microplate reader and cell viability was calculated. The inhibitory concentration-50 was obtained from the concentrations-inhibition response curve (n = 3).

4.2.3. Western blotting

4 T1-Luc2 cells (10^6 cells/well) were treated with tested compounds for 6 h, then collected using Trypsin-EDTA and centrifuged for 10 min at 2000 rpm, 4 °C. The supernatant was discarded and the cells were lysed in whole-cell lysis buffer (25 mmol/L HEPES, pH 7.7, 300 mmol/L NaCl, 1.5 mmol/L $MgCl_2$, 0.2 mmol/L EDTA, 0.1% Triton X-100, 20 mmol/L glycerophosphate, 1 mmol/L Na_3VO_4, 1 mmol/L phenylmethylsulfonyl fluoride, 1 mmol/L dithiothreitol, 10 mg/mL aprotinin, 10 mg/mL leupeptin). Cell lysates were subjected to electrophoresis in 10% SDS-PAGE, and electrophoretically transferred to Immobilon-P nylon membrane (Millipore, Bedford, MA, USA). The membranes were treated with Block Ace (Dainippon Pharmaceutical, Co. Ltd., Osaka, Japan) for at least 2 h, and probed with the indicated primary antibodies overnight, followed by horseradish peroxidase-conjugated secondary antibodies (1:1000 dilutions). Bands were visualized using ECL reagents (Amersham Bioscience, Piscataway, NJ, USA).

4.2.4. Colony formation assay

Cells in the exponential growth (3 × 105 cells/well) were plated in a 6-well plate and incubated overnight. After 24 h exposure to 10 ìM of 2a or 2d, the viable cells were counted and seeded into a 6-well plate in a range of 103 cells/well. The cells were then incubated for 10 days at 37 °C in a humidified 5% CO2 atmosphere. All the colonies were stained with 2% crystal violet.

4.2.5. IL-6 measurement

4 T1-Luc2 cells were cultured and treated with compound 2a, 2d (4, 8, 10 μM) or with the vehicle or for 24 h. Conditioned media from 4 T1-Luc2 cells were collected and centrifuged at 2,000 xg for 15 min at room temperature. The level of IL-6 in the supernatant was measured using commercially available enzyme-linked immunosorbent assay (ELISA) according to the manufacturer's instructions (BioLegend, California, USA). All data were corrected for total protein and expressed pg/mg protein.

4.3. Docking study

4.3.1. Ligand preparation

Different 3D conformations of the designed imidazole derivatives were generated and energetically minimized using the "Generate Conformations" tool in Discovery Studio (DS) 5.0 client (Accelrys). The lowest energetic conformation thus obtained was subjected to the "Prepare Ligands" module to generate its isomers at physiological pH. The CHARMM force field was employed to develop the partial atomic charges on each atom of the isomer. The isomer with the lowest CHARMM energy was used for the docking study.

4.3.2. Protein preparation and docking process.

The X-ray coordinates of STAT3 (pdb ID: 1BG1, resolution 2.25 Å) was retrieved from the protein data bank (www.rcsb.org). The "Prepare Protein" tool in DS was used to add missing atoms/chains and remove water molecules in the protein structure. The "Prepare Protein" algorithm was employed to protonate amino acid residues according to the physiological conditions. Determination of the binding site is accomplished by choosing the binding sphere covering the SH2 domain of STAT3. CDOCKER, a grid-based docking program, was used to dock the active compounds in the SH2 domain, considering the default parameters. The most favorable pose of the docked compounds was identified based on the CDOCKER energy (-CDE).

4.4. Optimization parameters LE and LLE.

The most active compounds were subjected to the prediction of drug-likeness and ligand-likeness scoring through some reliable measuring tools as LE and LLE. Molinspiration chemoinformatic server was used for the log*P* calculations [49].

Declaration of competing interest

The authors declare that they have no known competing financial interests or personal relationships that could have appeared to influence the work reported in this paper.

Appendix A. Supplementary material

Supplementary data to this article can be found online at https://doi.org/10.1016/j.bioorg.2021.105033.

References

[1] C.-Y. Loh, A. Arya, A.F. Naema, W.F. Wong, G. Sethi, C.Y. Looi, Signal transducer and activator of transcription (STATs) proteins in cancer and inflammation: Functions and therapeutic implication, Front. Oncol. 9 (2019) 48, https://doi.org/10.3389/fonc.2019.00048.

[2] B. Wingelhofer, H.A. Neubauer, P. Valent, X. Han, S.N. Constantinescu, P.T. Gunning, M. Müller, R. Moriggl, Implications of STAT3 and STAT5 signaling on gene regulation and chromatin remodeling in hematopoietic cancer, Leukemia 32 (2018) 1713–1726.

[3] G. Konjević, S. Radenković, A. Vuletić, M.M. Martinović, V. Jurišić, T. Srdić, STAT transcription factors in tumor development and targeted therapy of malignancies, Chapter 19, In *Oncogene and Cancer-From Bench to Clinic IntechOpen* (2013).

[4] H. Yu, R. Jove, The STATs of cancer–new molecular targets come of age, Nat. Rev. Cancer 4 (2004) 97–105.

[5] N.C. Reich, L. Liu, Tracking STAT nuclear traffic, *Nat.* Rev. *Immunol.* 6 (2006) 602–612.

[6] E. Bournazou, J. Bromberg, Targeting the tumor microenvironment, JAK-STAT3 signaling, *JAK-STAT* e23828 (2013).

[7] J.E. Darnell Jr., I.M. Kerr, G.R. Stark, Jak-STAT pathways and transcriptional activation in response to IFNs and other extracellular signaling proteins, Science 264 (1994) 1415–1421.

[8] R. Buettner, L.B. Mora, R. Jove, Activated STAT signaling in human tumors provides novel molecular targets for therapeutic intervention, Clin. Cancer Res. 8 (2002) 945–954.

[9] J. Bromberg, J.E. Darnell Jr., The role of STATs in transcriptional control and their impact on cellular function, Oncogene 19 (2000) 2468–2473.

[10] E.B. Haura, J. Turkson, R. Jove, Mechanisms of disease: Insights into the emerging role of signal transducers and activators of transcription in cancer, Nat. Clin. Pract. Oncol. 2 (2005) 315–324.

[11] H. Yu, D. Pardoll, R. Jove, STATs in cancer inflammation and immunity: a leading role for STAT3, Nat. Rev. Cancer. 9 (2009) 798–809.

[12] M. Benekli, H. Baumann, M. Wetzler, Targeting signal transducer and activator of transcription signaling pathway in leukemias, J. Clin. Oncol. 27 (2009) 4422–4432.

[13] R. Behera, V. Kumar, K. Lohite, S. Karnik, G.C. Kundu, Activation of JAK2/STAT3 signaling by osteopontin promotes tumor growth in human breast cancer cells, Carcinogenesis 31 (2010) 192–200.

[14] R.J. Leeman, V.W. Lui, J.R. Grandis, STAT3 as a therapeutic target in head and neck cancer, Expert. *Opin. Biol. Ther.* 6 (2006) 231–241.

[15] M. Kortylewski, R. Jove, H. Yu, Targeting STAT3 affects melanoma on multiple fronts, Cancer Metastasis Rev. 24 (2005) 315–327.

[16] M. He, C.Y. Young, New approaches to target the androgen receptor and STAT3 for prostate cancer treatments, Mini. Rev. Med. Chem. 9 (2009) 395–400.

[17] N. Wenta, H. Strauss, S. Meyer, U. Vinkemeier, Tyrosine phosphorylation regulates the partitioning of STAT1 between different dimer conformations, Proc. Natl. Acad. Sci. 105 (2008) 9238–9243.

[18] C.P. Lim, X. Cao, Structure, function, and regulation of STAT proteins, Mol. Biosyst. 2 (2006) 536–550.

[19] J. Sgrignani, S. Olsson, D. Ekonomiuk, D. Genini, R. Krause, C.V. Catapano, A. Cavalli, Molecular determinants for unphosphorylated STAT3 dimerization determined by integrative modeling, Biochemistry 54 (2015) 5489–5501.

[20] X. Chen, U. Vinkemeier, Y. Zhao, D. Jeruzalmi, J.E. Darnell, J. Kuriyan, Crystal structure of a tyrosine phosphorylated STAT-1 dimer bound to DNA, Cell 93 (1998) 827–839.

[21] F. Porta, G. Facchetti, N. Ferri, A. Gelain, F. Meneghetti, S. Villa, D. Barlocco, D. Masciocchi, A. Asai, N. Miyoshi, et al., An in vivo active 1,2,5-oxadiazole Pt(II) complex: A promising anticancer agent endowed with STAT3 inhibitory properties, Eur. J. Med. Chem. 131 (2017) 196–206.

[22] D. Masciocchi, A. Gelain, F. Porta, F. Meneghetti, A. Pedretti, G. Celentano, D. Barlocco, L. Legnani, L. Toma, B.-M. Kwon, A. Asai, S. Villa, Synthesis, structure-activity relationships and stereochemical investigations of new tricyclic pyridazinone derivatives as potential STAT3 inhibitors, Med. Chem. Comm. 4 (2013) 1181–1188.

[23] F. Porta, A. Gelain, D. Barlocco, N. Ferri, S. Marchiano, V. Cappello, L. Basile, S. Guccione, F. Meneghetti, S. Villa, A field-based disparity analysis of new 1,2,5-oxadiazole derivatives endowed with antiproliferative activity, Chem. Biol. Drug Des. 90 (2017) 820–839.

[24] F. Meneghetti, S. Villa, D. Masciocchi, D. Barlocco, L. Toma, D. Han, B. Kwon, N. Ogo, A. Asai, A. Gelain, L. Legnani, Ureido-pyridazinone derivatives: insights into the structural and conformational properties for STAT3 inhibition, Eur. J. Org. Chem. 2015 (2015) 4907–4912.

[25] M. Szelag, J. Wesoly, H.A. Bluyssen, Advances in peptidic and peptidomimetic-based approaches to inhibit STAT signaling in human diseases, Curr. Protein Pept. Sci. 17 (2016) 135–146.

[26] D. Masciocchi, S. Villa, F. Meneghetti, A. Pedretti, D. Barlocco, L. Legnani, L. Toma, B.-M. Kwon, S. Nakano, A. Asai, A. Gelain, Biological and computational evaluation of an oxadiazole derivative (MD77) as a new lead for direct STAT3 inhibitors, Med. Chem. Comm. 3 (2012) 592–599.

[27] D.S. Shin, D. Masciocchi, A. Gelain, S. Villa, D. Barlocco, F. Meneghetti, A. Pedretti, Y.M. Han, D.C. Han, B.M. Kwon, L. Legnani, Synthesis, modeling, and crystallographic study of 3,4-disubstituted-1,2,5-oxadiazoles and evaluation of their ability to decrease STAT3 activity, Med. Chem. Comm. 1 (2010) 156–164.

[28] G. Poli, A. Gelain, F. Porta, A. Asai, A. Martinelli, T. Tuccinardi, Identification of a new STAT3 dimerization inhibitor through a pharmacophore-based virtual screening approach, J. Enz. Inhib. Med. Chem. 3 (2016) 1011–1017.

[29] I. Ali, M.N. Lone, H.Y. Aboul-Enein, Imidazoles as potential anticancer agents, Med. Chem. Commun. 8 (2017) 1742–1773.

[30] H.D. Dakin, R. West, A general reaction of amino acids, J. Biol. Chem. 78 (1928) 91–104.

[31] Y.M. Loksha, P.T. Jørgensen, E.B. Pedersen, Synthesis of imidazoles as novel emivirine and S-DABO analogues, J. Heterocyclic Chem. 39 (2002) 375–382.

[32] Y.M. Loksha, M.A. El-Badawib, A.A. El-Barbaryb, E.B. Pedersen, C. Nielsenc, Synthesis of 2-Hydroxymethyl-1H-imidazole from 1,3-Dihydroimidazole-2-thiones, Synthesis 1 (2004) 116–120.

[33] T. Migita, T. Shimizu, Y. Asami, J. Shiobara, Y. Kato, M. Kosugi, The palladium catalyzed nucleophilic substitution of aryl halides by thiolate anions, Bull. Chem. Soc. Jpn. 53 (1980) 1385–1389.

[34] M. Ko-sugi, T. Ogata, M. Terada, H. Sano, T. Migita, Palladium-catalyzed reaction of stannyl sulfide with aryl bromide. Preparation of aryl sulfide, Bull. Chem. Soc. Jpn. 58 (1985) 3657–3658.

[35] L. Rout, P. Saha, S. Jammi, T. Punniyamurthy, Efficient copper (I)-catalyzed C-S cross coupling of thiols with aryl halides in water, Eur. J. Org. Chem. 2008 (2008) 640–643.

[36] A.S. Salman, A. Abdel-Aziem, M.J.S. Alkubbat, Design, Synthesis of some new thiosubstituted imidazole and their biological activity, Am. J. Org. Chem. 5 (2015) 57–72.

[37] D. Mishra, R. Singh, C. Rout, A facile amidation of chloroacetyl chloride using DBU, Int. J. Chem. Tech. Res. 10 (2017) 365–372.

[38] A.S. Salman, A. Abdel-Aziem, M.J.S. Alkubbat, Synthesis, spectroscopic characterization and antimicrobial activity of some new 2-substituted imidazole derivatives, Int. J. Org. Chem. 5 (2015) 15–28.

[39] M.A. Taha, S.M. El-Badryanhydrous, Antimicrobial assessment of some heterocyclic compounds utilizing ethyl 1-aminotetrazole-5-carboxylate, J. Korean Chem. Soc. 54 (2010) 414–418.

[40] M. Szelag, K. Sikorski, A. Czerwoniec, K. Szatkowska, J. Wesoly, H.A. Bluyssen, In silico simulations of STAT1 and STAT3 inhibitors predict SH2 domain cross-binding specificity, Eur. J. Pharmacol. 720 (2013) 38–48.

[41] T. Li, W. Wang, H. Chen, T. Li, L. Ye, Evaluation of anti-leukemia effect of resveratrol by modulating STAT3 signaling, Int, Immunopharmacol. 10 (2010) 18–25.

[42] S. Becker, B. Groner, C.W. Müller, Three-dimensional structure of the Stat3β homodimer bound to DNA, Nature 394 (1998) 145–151.

[43] Dassault Systèmes BIOVIA, Discovery Studio Modeling Environment, Release 2019, Dassault Systèmes, San Diego, 2016.

[44] Y. Wang, X. Ren, C. Deng, L. Yang, E. Yan, T. Guo, Y. Li, M.X. Xu, Mechanism of the inhibition of the STAT3 signaling pathway by EGCG, *Oncol. Rep.* 30 (2013) 2691–2696.

[45] T. Zhang, W.H. Kee, K.T. Seow, W. Fung, X. Cao, The coiled-coil domain of Stat3 is essential for its SH2 domain-mediated receptor binding and subsequent activation induced by epidermal growth factor and interleukin-6, Mol. Cell. Biol. 20 (2000) 7132–7139.

[46] S. Schultes, C. de Graaf, E.E.J. Haaksma, I.J.P. de Esch, R. Leurs, O. Krämer, Ligand efficiency as a guide in fragment hit selection and optimization, Drug Discov. 7 (2010) e157–e162.

[47] J.A. Arnott, S.L. Planey, R. Kumar, Lipophilicity indices for drug development, J. Appl. Biopharm. Pharmacokinet. 1 (2013) 31–36.

[48] A.L. Hopkins, G.M. Keserü, P.D. Leeson, D.C. Rees, C.H. Reynolds, The role of ligand efficiency metrics in drug discovery, Nat. Rev. Drug Discov. 13 (2014) 105–121.

[49] http://www.molinspiration.com (Accessed 6:00 pm, March 10, 2019).